A Monte Carlo-based modeling method for the spatial-temporal evolution process of multi-hazard and higher-order domino effect

Ma, Weikai; Wang, Yanfu; Xing, Peijie; Yang, Ming

DOI
10.1016/j.ress.2024.110532

Publication date
2025

Document Version
Final published version

Published in
Reliability Engineering and System Safety

Citation (APA)
Ma, W., Wang, Y., Xing, P., & Yang, M. (2025). A Monte Carlo-based modeling method for the spatial-temporal evolution process of multi-hazard and higher-order domino effect. *Reliability Engineering and System Safety*, *253*, Article 110532. https://doi.org/10.1016/j.ress.2024.110532

Reliability Engineering and System Safety 253 (2025) 110532

Contents lists available at ScienceDirect

Reliability Engineering and System Safety

journal homepage: www.elsevier.com/locate/ress

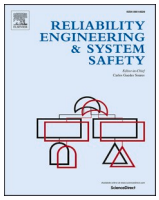

A Monte Carlo-based modeling method for the spatial-temporal evolution process of multi-hazard and higher-order domino effect

Weikai Ma [a], Yanfu Wang [a,*], Peijie Xing [a], Ming Yang [b]

[a] Department of Safety Science and Engineering, College of Mechanical and Electronic, Engineering, China University of Petroleum, Qingdao 266580, PR China
[b] Safety and Security Science Section, Faculty of Technology, Policy and Management, TU Delft, Delft, the Netherlands

ARTICLE INFO

Keywords:
Domino effect
Uncertainty
Monte Carlo method
Spatial-temporal evolution

ABSTRACT

The domino effect in chemical industrial parks represents a complex phenomenon where accidents such as leaks, fires, and explosions can occur either simultaneously or in sequence. The progression of domino accidents is highly uncertain, making it difficult to anticipate the spatial-temporal development of such accidents. This paper presents a model that aims to forecast the evolution of domino effects by considering the critical thermal dose and utilizing the Probit model to assess the escalation of incidents caused by thermal radiation and overpressure. To tackle the complexities associated with multiple installations, high order, and various accident types in modeling domino effect accidents, the model incorporates Monte Carlo simulation methods. The model validation and case studies have demonstrated the effectiveness of this approach in simulating the progression of domino accidents initiated by a range of primary accidents. This approach enables the prediction of potential accident chains and the dynamic failure probability of hazardous installations, including the identification of the initial installation likely to fail. The insights gained from this research offer guidance for the prevention and mitigation of the domino effect in chemical accidents.

1. Introduction

In chemical industry parks, hazards such as leakage, fire, and explosion arising from loss of containment (LOC) may occur due to various reasons [1]. In the chemical industry, the interconnected nature of installations has made process safety management a critical concern [2,3]. The potential for a fire or explosion to cause damage to nearby facilities, leading to a chain reaction of escalating events, is commonly referred to as the 'domino effect'. These accidents, while rare, can have significant and unpredictable consequences [4-7].

Typical domino accidents, such as Buncefield oil depot explosion in the UK in 2005, the Caribbean Petroleum Corporation fire and explosion in Puerto Rico in 2009, and the Intercontinental Terminal Company Deer Park fire in the USA in 2009, highlight the temporal and spatial propagation characteristics of the domino effect, particularly in scenarios involving storage tanks storing hazardous materials in close proximity [8-12].

The complexity and uncertainty of domino accidents underscore the critical need for accident forecasting and risk assessment in the chemical process industry [13,14]. Researchers have identified two main sources of uncertainty in predicting domino effects: parameter uncertainty related to accident scenarios and escalation probabilities, and model uncertainty related to event sequence modeling [13]. The evolution of a domino accident can be further complicated by the occurrence of multiple primary accident scenarios and the superposition of multiple physical effects on a target installation [15,16].

Various modeling approaches have been used to study the uncertainty of the domino effect including threshold modeling for identifying potentially damaged installations. However, threshold model cannot quantitatively determine the probability of domino effect [5]. The Probit model obtained by fitting probabilistic analysis methods based on statistical analysis is widely used to quantitatively assess the calculation of industrial risk from domino accidents, particularly those involving thermal radiation and overpressure [17,18]. The Probit model combines the damage probability with time to failure (TTF). Thus, the probit model overcomes the limitations presented by threshold-based approach. Recently, Marroni et al. [19] developed fragility models for improvised explosives, firearms and incendiary weapons, expanding the applications of probabilistic modelling.

Dynamic modeling techniques, such as dynamic Bayesian network approach [4,13,20,21], dynamic graph approach [10,22,23], Petri-net [24-26], copula theory [3,27] agent-based modeling approach

* Corresponding author.
E-mail address: wangyanfu@upc.edu.cn (Y. Wang).

https://doi.org/10.1016/j.ress.2024.110532
Received 28 January 2024; Received in revised form 18 August 2024; Accepted 30 September 2024
Available online 4 October 2024

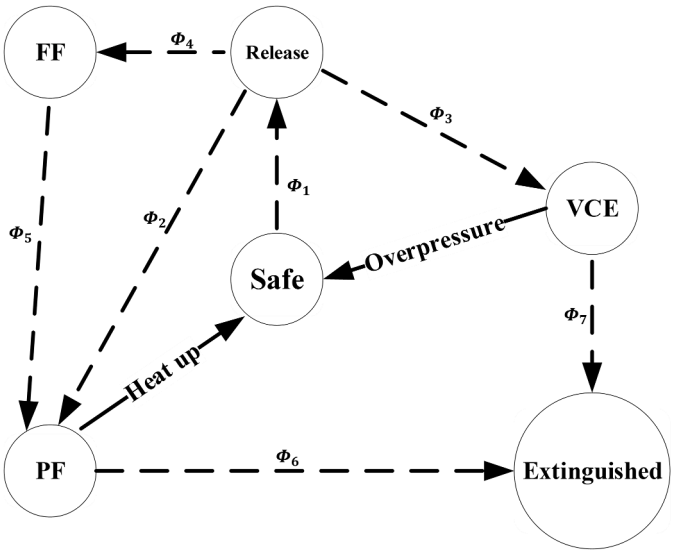

Fig. 1. State transition and escalation vectors.

[28-32], Monte Carlo simulation [1,6,33-36] and Markov chain [37] are common tools used in process reliability analysis [38]. While graphical methods can simplify the modeling of higher-order domino effects, they may face limitations in complex industrial systems [14]. For instance, the application can become challenging when using Bayesian methods to model multiple installations due to the voluminous conditional probability tables involved. Suppose the uncertainty in hazard evolution is taken into consideration, the graph's structure will become more complex and even require the establishment of multiple graphs to represent multiple accident chains [39]. Alternative approaches focusing on states and state transition rules for basic units, such as agent-based modeling approach, Monte Carlo simulation, offer additional tools for addressing uncertainties in hazard evolution and assessing the safety risks of process systems. Despite the time-consuming nature of some modeling methods, such as Monte Carlo simulation, these approaches are valuable for reducing the complexities of mathematical calculations and improving the understanding of domino accidents in the chemical industry [31]. Subsequent research has further expanded the applicability and flexibility of Monte Carlo simulation in addressing the uncertainty, complexity, and time-dependency associated with domino effects [6,33,35]. When modeling domino evolution for complex systems with numerous of installations, the advantages of Monte Carlo methods over graph methods become more evident.

Computational Fluid Dynamics (CFD) and Finite Element Analysis (FEA) have been utilized in modeling domino effects due to their ability to simulate physical effects effectively. Initially, researchers used CFD to predict the thermal radiation distribution on the target tank surface, then combined with the Probit model to assess the likelihood of secondary accidents [40]. Additionally, thermal radiation was used as the heat load in FEA to analyze the thermal response process, simulate temperature and stress distribution on the tank surface, and determine the tank's failure time [41-43]. While coupling CFD and FEA modeling can provide more accurate results on physical effects and aid in vulnerability assessment, it is complex, time-consuming, and expensive [39]. To address time constraints, some researchers have developed analytical functions based on FEA or simulation results to predict failure time, and fire scenarios [5, 44-47]. These results have also been used to develop machine learning-based methods for dynamic domino effect assessment. For instance, random forest and neural network models have been employed to predict yield strength during fire exposure and quantify the TTF of atmospheric storage tanks [9,48]. However, current research methods still have limitations in practical application when dealing with the time-dependency and multifaceted interactions of higher-order domino effects.

When modeling the evolution process of the domino effect using Bayesian or Monte Carlo methods, relying on the basic Probit model may underestimate the associated risk, especially when considering thermal radiation below the escalation threshold for tank shell strength. To address these limitations, the concept of "thermal dose" has emerged as a rapid alternative for higher-order domino effects with variable radiation sources. Recent studies have introduced the concept of "critical thermal dose" to evaluate the failure time of target installations exposed to multiple fires [26,49-51] and to assess the probability of domino effects [52]. However, current research primarily focuses on the evolution of domino effects related to single accident types, neglecting the combined effects of thermal radiation and overpressure that may occur simultaneously. This increases the likelihood of a sequential failure and the simultaneous presence of multiple physical effects, thereby increasing the uncertainty in predicting the probability and evolution path of domino accidents [5,7,16,49,53,54].

In conclusion, there is a need for a comprehensive and practical accident evolution model for multi-devices and high-order domino scenarios, considering the uncertainty of dynamic evolution processes of multiple hazardous types. This study uses critical thermal dose as the failure criterion for tanks exposed to fire and employs the Monte Carlo simulation method to establish a spatial-temporal evolution model of domino effect. This improvement helps to overcome the underestimation of thermal radiation's ability to cause domino effects in traditional methods. It provides more detailed insights into the evolution of domino effects, focusing on the higher-order evolution of multiple accident types. This aims to enhance safety and emergency management in complex chemical industrial environments.

This paper is organized as follows. In Section 2, the accident escalation rules during the evolution of the domino effect are analyzed. Section 3 demonstrates the computational logic of the model, especially how to use the Monte Carlo method to deal with the uncertainty of ignition and the evolution of different hazards. In Section 4, the reliability and accuracy of the model through the Buncefield accident is verified. In Section 5, a case study is demonstrated to show the application of the developed model. Section 6 concludes the study.

2. Evolutionary rules of domino effect

2.1. Accident state

As outlined in the event trees presented by Vílchez et al. [55], hazardous installations in chemical industry parks may be in the state of safe, release (RE), pool fire (PF), vapor cloud explosion (VCE), and flash fire (FF) during the accident evolution. The different states involved in this evolution and the physical effects that trigger these transitions can be observed in Fig. 1. In this figure, dotted lines indicate state transition between nodes, and solid lines represent physical effects caused by one node on other nodes. Events $\varphi_1 - \varphi_7$ are identified as the triggers for these state transitions.

Installations exposed to PF or VCE may transit from safe state to failed state, and LOC is widely recognized as the most frequent initiating event in the accident sequence (φ_1). In the domino effect triggered by fires, there is typically a time-lapse occurs between the start of primary and secondary events, whereas for other escalation vectors like overpressure, the secondary scenarios occur almost simultaneously with the primary event [56]. After analyzing over 100 domino accidents, Cozzani [57] pointed out that FF normally did not cause domino escalation, because the limited duration of FF reduces its escalation effect [58]. PF will occur if the released materials are immediately ignited (φ_2). If delayed ignition occurs, it may lead to VCE (φ_3) or FF (φ_4). After FF, the state immediately changes to PF (φ_5). After the fuel is burnt out or a VCE occurs, the state changes to extinguished (φ_6, φ_7) [1,8,35,59]. Ignitions caused by different ignition sources are considered as independent events. The Purple Book [59] and BEVI Reference Manual [60] provide information on the direct ignition probability (P_1) for various released substances. In the evolution of the

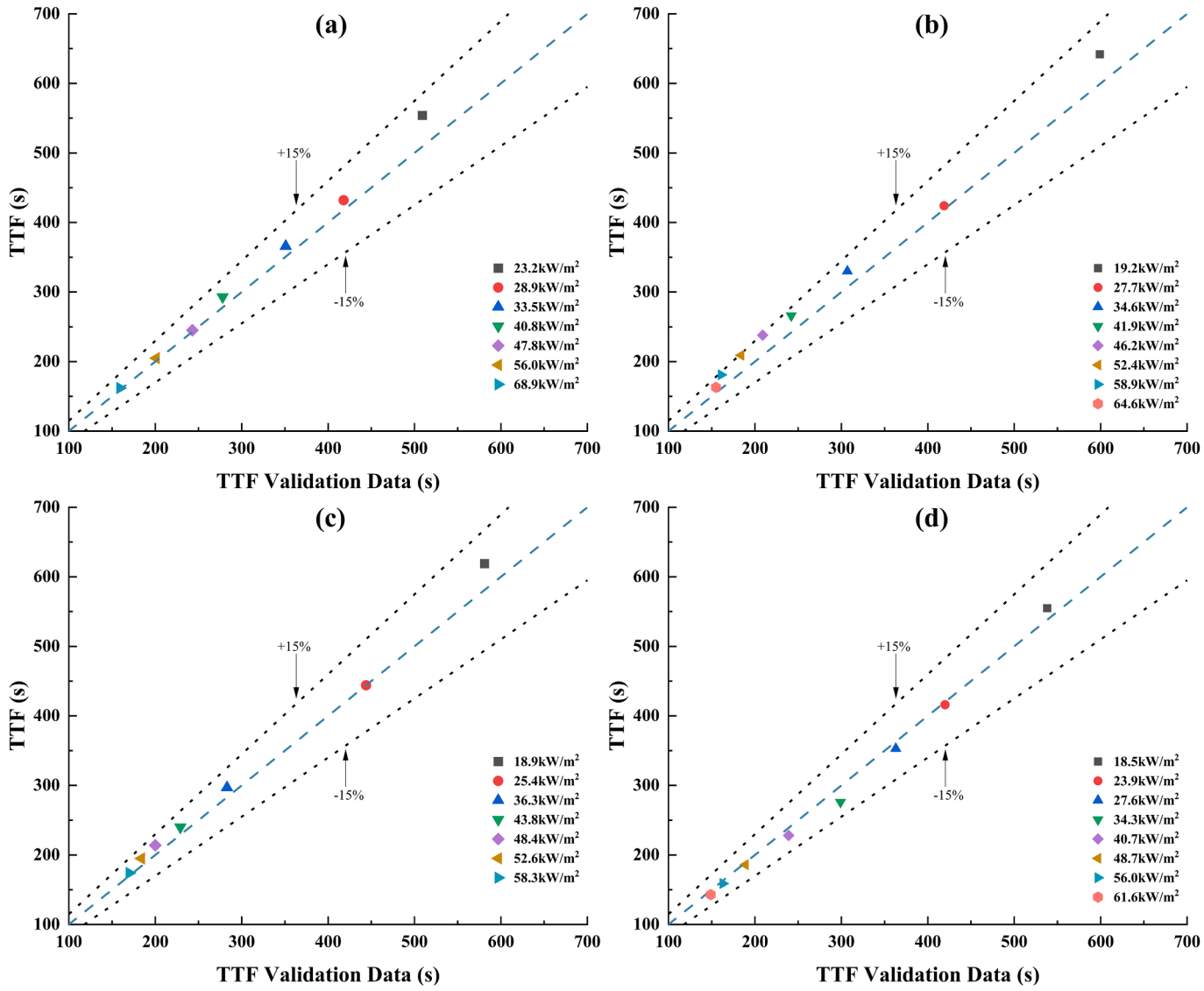

Fig. 2. Comparison of TTF in the literature with the results of Yang's results (a.500m^3, b.3000m^3 c.5000m^3, d.10000m^3).

domino effect, the direct ignition probability after failure due to thermal radiation is $P_1^{'}$. In contrast, the failure resulting from overpressure causes the instantaneous release of all contents with a direct ignition probability of $P_1^{''}$. Furthermore, the probability of a vapor cloud being ignited within one minute is approximately 1 when there are many ignition sources nearby [59]. The probability of VCE or FF caused by the delayed ignition is P_2 and P_3, respectively. And the delayed ignition probability can be determined through Eq. (1) [59,60].

$$P_{IS}(t_{IS}) = 1 - e^{-\omega t_{IS}} \tag{1}$$

where, $P_{IS}(t)$ is the cumulative ignition probability caused by ignition source IS within the time range between 0 and t. ω (s^{-1}) is the ignition efficiency, which is related to the ignition characteristics. t_{IS} (s) represents the time that ignition source IS is covered by the vapor cloud. To determine t_{IS}, the vapor cloud dispersion model can be adopted, as Eq. (2) [61]:

$$R_t = \left(\frac{4}{3}\right)^{0.75} \times {c_E}^{0.5} \times \left(\frac{\rho}{2\pi}\right)^{0.25} \times {V_c}^{0.25} \times t^{0.75} \tag{2}$$

where R_t is the radius of the area in which cloud might be ignited at time t; c_E is an empirical constant approximately equal to 1; V_c is the volume flow rate of the flammable gas; ρ is the vapor density relative to air. This dispersion model is suitable for low-wind conditions and neglects the effects of obstacles on dispersion.

2.2. Determination of accident escalation

As mentioned above, the domino effect triggered by PF and VCE is studied in this paper. Whether thermal radiation leads to the installation failure is determined based on the critical thermal dose, and the Probit model can be used to determine the damage probability of target installations due to overpressure.

For the analysis of fire-induced domino effects, Eqs. (3) and (4) are often used to estimate the TTF of target installations [57]:

$$\text{Atmospheric installation}: \ln(\text{TTF}) = -1.128 \times \ln(Q) - 2.667 \times 10^{-5} \times V + 9.877 \tag{3}$$

$$\text{Pressurized installation}: \ln(\text{TTF}) = -0.947 \times \ln(Q) - 8.835 \times V^{0.032} \tag{4}$$

where, Q (kW/m^2) is the thermal radiation intensity, V (m^3) is the volume of the installation, and the unit of TTF is second.

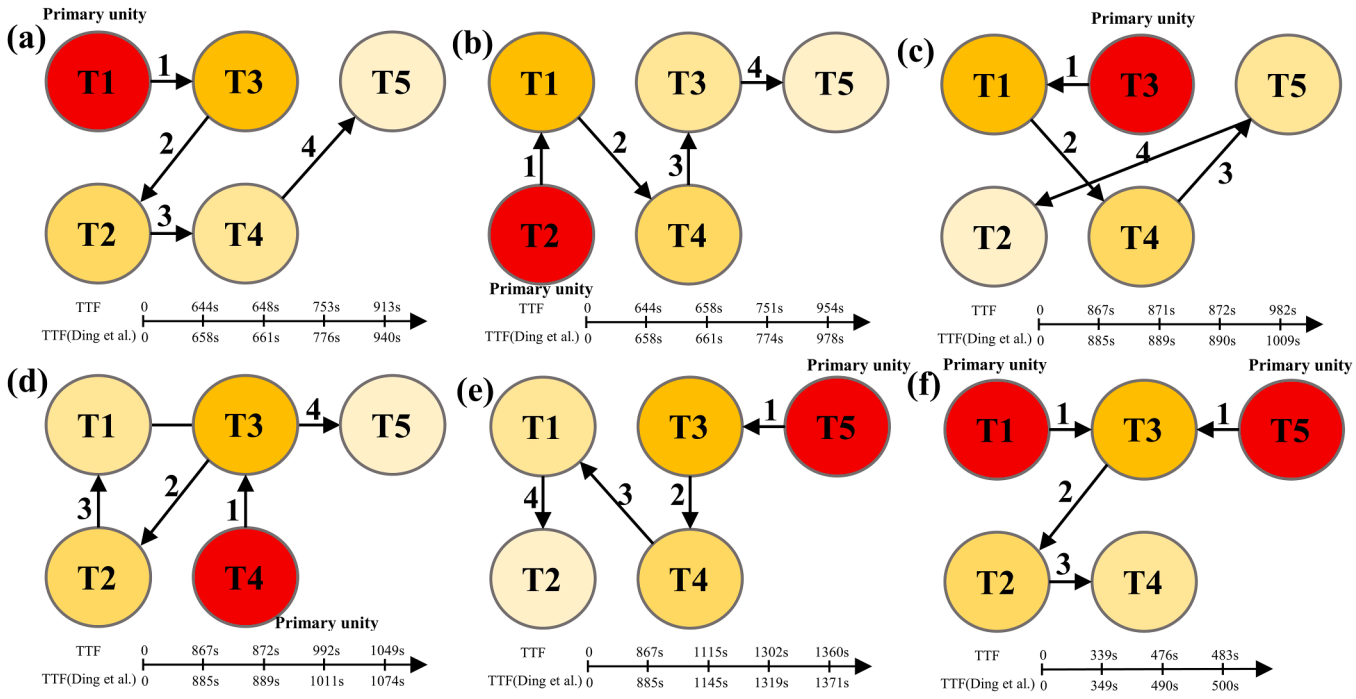

Fig. 3. Comparison of failure time of tanks in domino evolution process calculated by current model and Ding et al.

Table 1
Heat radiation intensity (kW/m^2).

		Tank j				
		T1	T2	T3	T4	T5
Tank i	T1	–	20.3	20.3	12.3	6.7
	T2	20.3	–	12.3	20.3	5.4
	T3	15.6	9.0	–	15.6	15.6
	T4	9.0	15.6	15.6	–	9.0
	T5	4.7	3.8	15.6	9.0	–

According to Eqs. (3) and (4), the critical thermal dose (D_{th}) that causes the failure of installation is defined as follows [26,51]:

$$D_{th} = Q^{\alpha} \times \ TTF \tag{5}$$

where, α is a constant. The critical thermal dose is determined using Eqs. (6) and (7):

$$\text{Atmospheric vessels}: \ D_{th} = Q^{1.128} \times \ TTF = e^{-\left(2.667 \times 10^{-5} \times V - 9.877\right)} \tag{6}$$

$$\text{Pressurized vessels}: \ D_{th} = Q^{0.947} \times \ TTF = e^{-\left(8.835 \times V^{0.032}\right)} \tag{7}$$

When analyzing the domino effect, the volume of the target installation is constant. Thus, D_{th} can be regarded as a constant, representing a threshold for the failure of the target installation due to the accumulation of heat.

In Zhou's study, the accuracy of Eqs. (6) and (7) was not validated. Yang et al. [46] determined the TTFs of atmospheric tanks exposed to fire using FEA. In this paper, Yang's findings are used to validate Eqs. (6) and (7). As illustrated in Fig. 2, the results obtained by applying the equations closely match the verification results when the tanks are subjected to varying levels of thermal radiation, with nearly all results showing an error margin of less than 15%.

Fig. 3 illustrates a comparison of the accident escalation sequence and time under different primary scenarios calculated using Eq. (5) to Eq. (7) with the research conducted by Ding et al. [50] when considering the accumulation of thermal dose. In this comparison, six primary accident scenarios are simulated: primary PF occur on tanks T1-T5, and simultaneous PFs occur on T1 and T5. It is evident that the domino accident sequence and the individual tank failure times derived from Eq. (5) to Eq. (7) are consistent with the published results, with a maximum deviation of 3.4%. In this case, atmospheric tanks T1-T5 have volumes of 500m^3, 200 m^3, 500 m^3, 200 m^3, and 200 m^3 respectively. Table 1 lists heat radiation intensity released by tank i on tank j.

Cozzani [58,62] provided a summary of Probit models and explosion overpressure threshold P_{th} for each category of installation (atmospheric, pressurized, elongated and small). This study utilizes these specific Probit models to assess the probability of damage to installations resulting from overpressure. Generally, the Probit model can be expressed as Eqs. (8)- (11):

$$\text{Atmospheric vessels}: \ Y = -18.94 + 2.44\ln(\Delta P) \tag{8}$$

$$\text{Pressurized vessels}: \ Y = -42.44 + 4.33\ln(\Delta P) \tag{9}$$

$$\text{Elongated equipment}: \ Y = -28.07 + 3.16\ln(\Delta P) \tag{10}$$

$$\text{Small equipment}: \ Y = -17.79 + 2.18\ln(\Delta P) \tag{11}$$

where, Y is the Probit value; a and b are coefficients; and ΔP(kPa) is the is the peak overpressure. After Y is obtained, the escalation probability P can be calculated using the cumulative standard normal distribution, as shown in Eq. (12):

$$P = \frac{1}{\sqrt{2\pi}} \int_{-\infty}^{Y-5} e^{-\frac{u^2}{2}} du \tag{12}$$

3. Spatial-temporal evolution model of domino effect

The main modeling steps include collecting basic information, setting parameters, slecting primary accidents, and analyzing the evolution process and failure probability through matrix calculations combined with Monte Carlo methods.

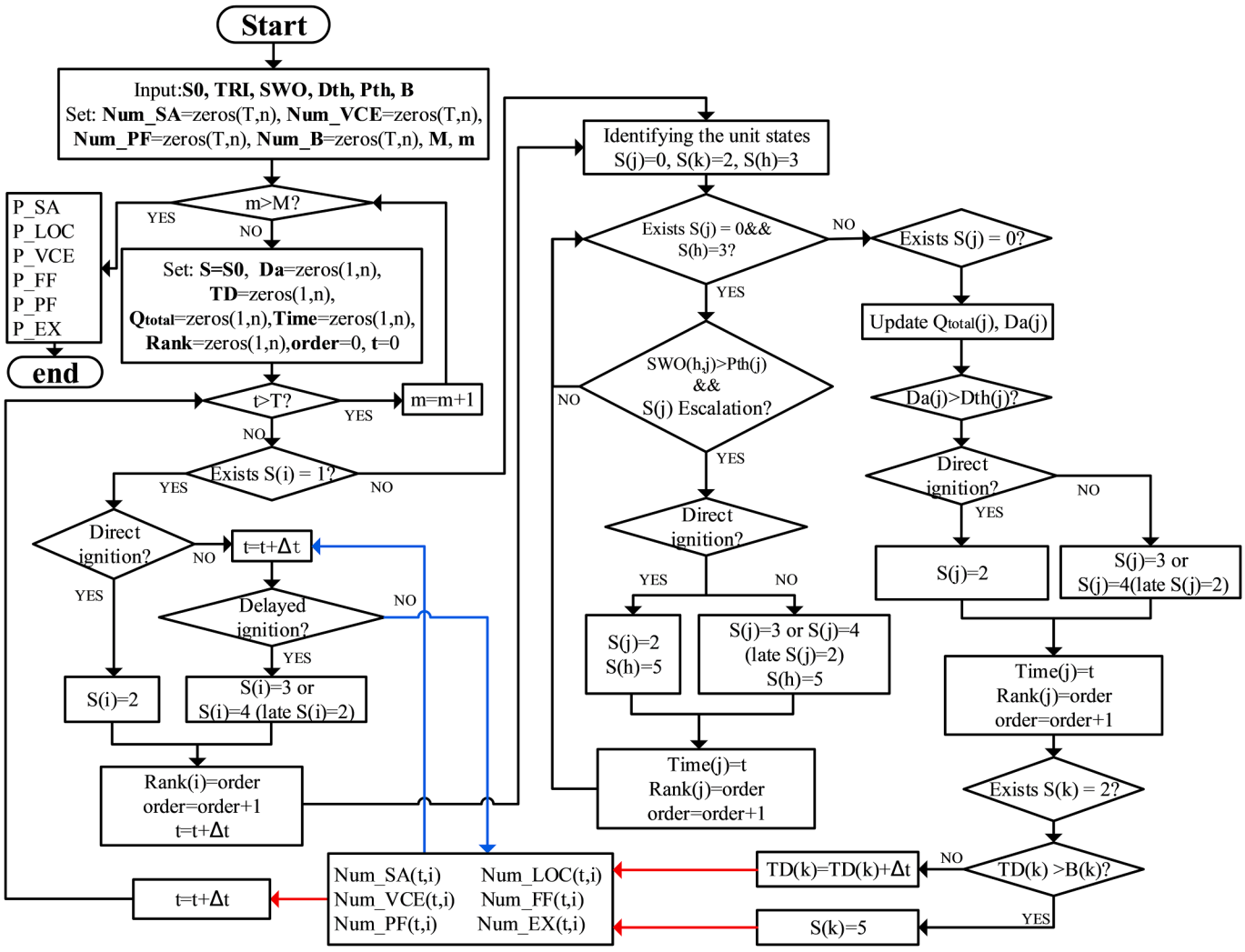

Fig. 4. Flowchart of the algorithm for the spatial-temporal evolution model of domino effect (The blue and red lines represent different program processes).

3.1. Collecting basic information

The relevant information about the chemical industry will function as the input of the model or serve as the foundation of parameter calculation. The detailed information are as follows:

Plant Layout: This includes the position of installations and the distances between different installations.

Installation Data: This encompasses the type and size of the installation, as well as the characteristics and quantities of the hazardous materials stored.

Environmental Parameters: The ambient temperature, humidity, wind speed and wind direction at the time of the accident.

3.2. Calculating and setting parameters

Installations with the potential for domino effect escalation can be considered as nodes [35,63]. The state of each node is closely related to time factors, and at a point during the evolution process, the nodes may be in one of six states: safety, release, PF, VCE, FF, and extinguished, as analyzed in the Section 2.1. For a system with **n** installations, the states of each node can be represented by the matrix **S**, a state matrix of $1 \times n$ is obtained as Eq. (13):

$$S = [\, s_1 \quad s_2 \quad \cdots \quad s_n \,] \tag{13}$$

where s_i represents the state of installation i, and the values are given by Eq. (14):

$$s_i = \begin{cases} 0 & \textit{safe state} \\ 1 & \textit{Release state} \\ 2 & \textit{PF state} \\ 3 & \textit{VCE state} \\ 4 & \textit{FF state} \\ 5 & \textit{Extinguished state} \end{cases} \tag{14}$$

The thermal radiation values and explosion overpressure values between installations are converted to $n \times n$ dimensional matrices **TRI** and **SWO**, given by Eqs. (15) and (16):

$$TRI = \begin{bmatrix} 0 & q_{12} & \cdots & q_{1n} \\ q_{21} & 0 & \cdots & q_{2n} \\ \cdots & \cdots & 0 & \cdots \\ q_{n1} & q_{n2} & \cdots & 0 \end{bmatrix} \tag{15}$$

$$SWO = \begin{bmatrix} 0 & p_{S12} & \cdots & p_{s1n} \\ p_{s21} & 0 & \cdots & p_{s2n} \\ \cdots & \cdots & 0 & \cdots \\ p_{sn1} & p_{sn2} & \cdots & 0 \end{bmatrix} \tag{16}$$

$q_{ij}(kW/m^2)$ represents the thermal radiation of installation i to

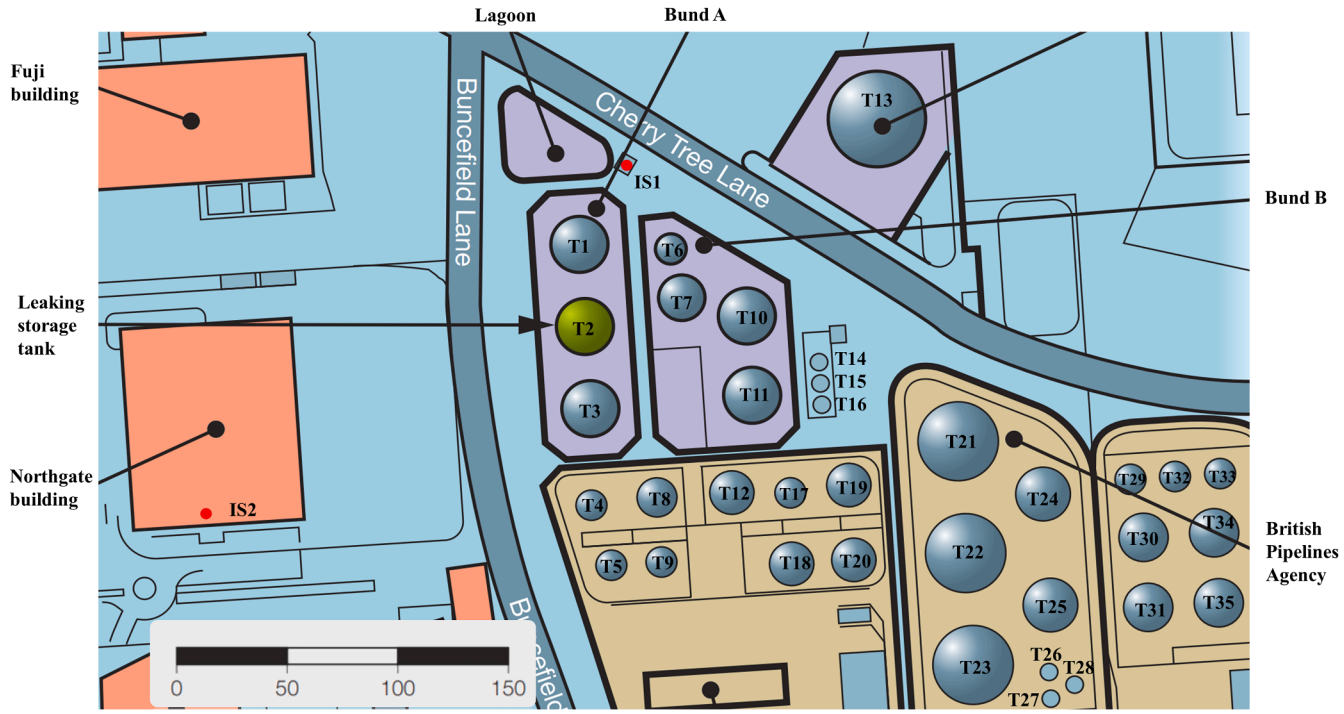

Fig. 5. The layout of the Buncefield oil storage and transfer depot [67].

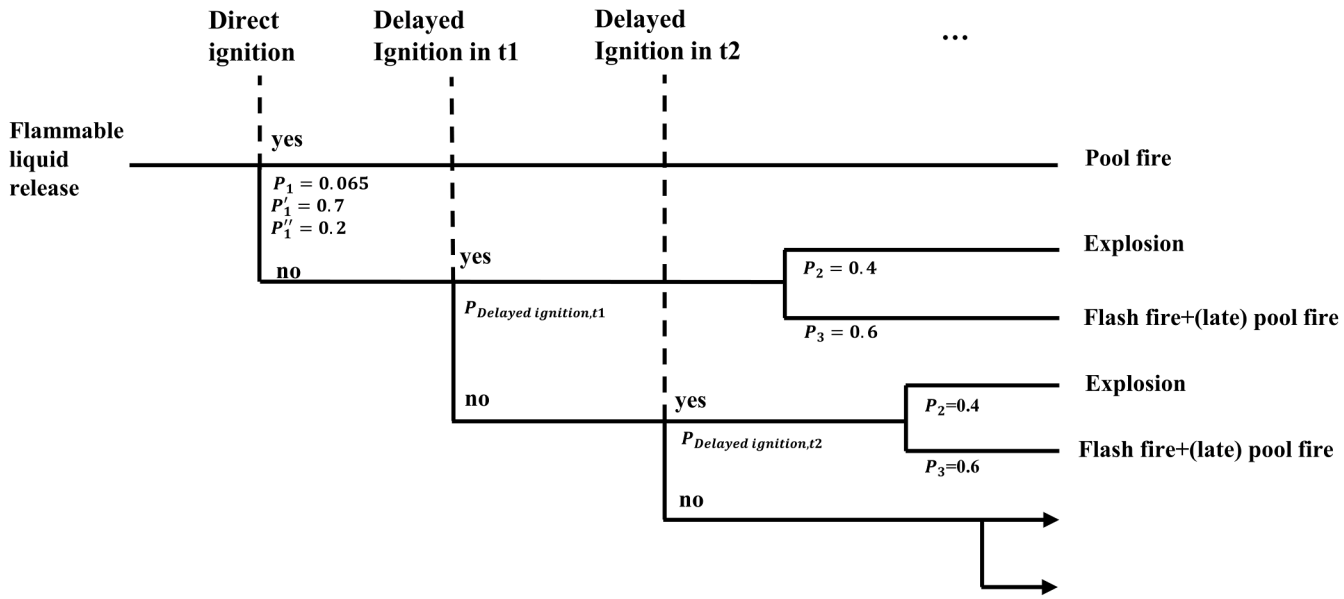

Fig. 6. Simplified event tree for flammable liquid and volatile leakage.

installation j ($i \in \{1,2,\cdots,n\}, j \in \{1,2,\cdots,n\}$). Moreover, p_{sij} (kPa) represents the overpressure of installation i to installation j ($i \in \{1,2,\cdots,n\}$, $j \in \{1,2,\cdots,n\}$).

Mathematical models and simulation software are usually used to determine thermal radiation and explosion overpressure. The solid flame model is often used to calculate the thermal radiation of PF, and the commonly used overpressure estimation methods include the TNT equivalent method and TNO Multi-Energy method [64]. Assael and Kakosimos [65] provided a detailed introduction to the usage of mathematical models. Simulation software, such as PHAST and ALOHA, is also used tosimulate the consequences of industrial accidents and provide for the analysis of combustion and explosion [66].

Meanwhile, according to Eqs. (5) and (6), the critical thermal dose of the hazardous installations can be calculated to obtain the $1 \times n$ dimensional matrix **Dth** as shown in Eq. (17)

$$\mathrm{Dth} = [\ \mathrm{Dth}_1 \quad \mathrm{Dth}_2 \quad \cdots \quad \mathrm{Dth}_n\ ] \tag{17}$$

In addition, **Pth**: $1 \times n$ dimensional matrix, the element Pth_i represents the threshold of explosion overpressure of installation i ($i \in \{1,2,\cdots,n\}$) as shown in Eq. (18); For atmospheric vessels, the failure threshold is 22 kPa, and for pressurized vessels, the failure threshold is 16 kPa. **B**: $1 \times n$ dimensional matrix, the element B_i represents the duration after the fire of installation i ($i \in \{1,2,\cdots,n\}$) as shown in Eq. (19).

$$\mathrm{Pth} = [\ \mathrm{Pth}_1 \quad \mathrm{Pth}_2 \quad \cdots \quad \mathrm{Pth}_n\ ] \tag{18}$$

$$\mathrm{B} = [\ \mathrm{B}_1 \quad \mathrm{B}_2 \quad \cdots \quad \mathrm{B}_n\ ] \tag{19}$$

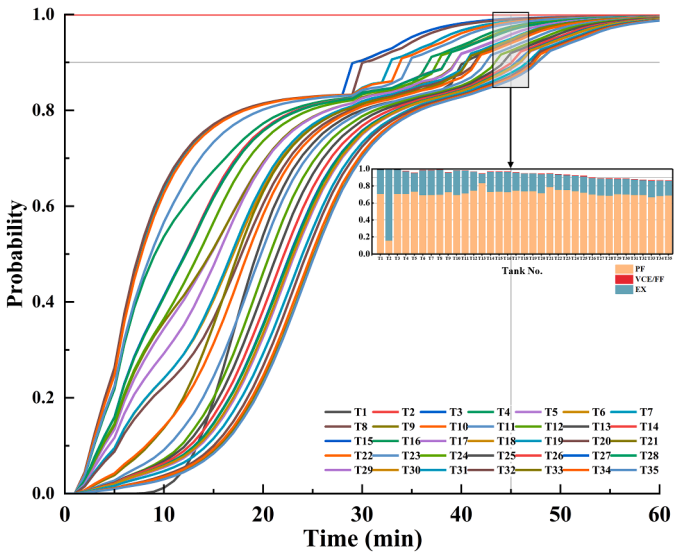

Fig. 7. Dynamic failure probability of tanks.

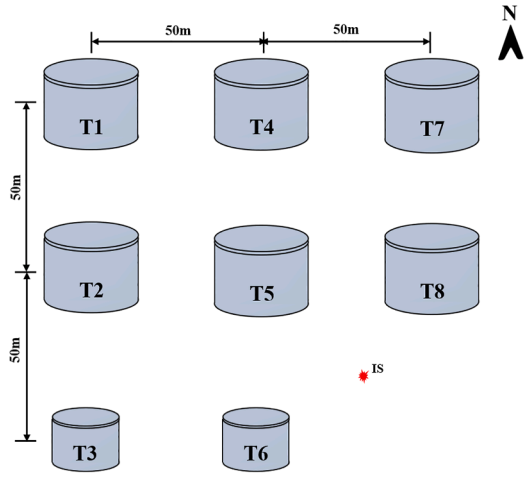

Fig. 8. Schematic layout of the tanks.

Table 2
Parameters of each tank [35].

Tank No.	Chemical substance	Type	Size (diameter × height)	Volume (m^3)
T1	Benzene	Atmospheric	18.2 m × 12.59m	3000
T2	Benzene	Atmospheric	18.2 m × 12.59m	3000
T3	Toluene	Atmospheric	8.45 m × 8.92m	500
T4	Benzene	Atmospheric	18.2 m × 12.59m	3000
T5	Benzene	Atmospheric	18.2 m × 12.59m	3000
T6	Toluene	Atmospheric	8.45 m × 8.92m	500
T7	Benzene	Atmospheric	18.2 m × 12.59m	3000
T8	Benzene	Atmospheric	18.2 m × 12.59m	3000

3.3. Modeling procedure

The detailed calculation flow of the spatial-temporal evolution model of domino effect proposed in this study is shown in Fig. 4 and explained as follows:

3.3.1. Establishing initial conditions and initializing parameters

Set the primary accident scenario **S0** and input parameters **TRI, SWO, Dth, Pth**, and **B**. Set temporary parameters **Num_SA, Num_RE, Num_PF, Num_VCE**, and **Num_EX** with initial values 0, these parameters are all T×n dimensional matrices used to calculate dynamic probabilities. Monte Carlo simulation starts from $\boldsymbol{m} = 1$, and the number of iterations is **M**.

3.3.2. Conducting Monte Carlo simulations

At the beginning of each iteration, whether the variable 'm' has reached the value of 'M' is checked. If it has, this signifies the end of the simulation. If not, the specific parameters are reset and a new iteration starts. The parameters that need to be reset include **Da**, which represents the cumulative heat dose for each installation in the safe state; **TD,**which represents the duration time of each installation in the PF state; $\mathbf{Q_{total}}$, which represents the thermal radiation intensity received of each installation; **Time**, which is used to record the escalation time of each installation; **Rank**, which is used to record the escalation order of each installation. All of these are 1×n dimensional matrices with initial values of 0. The state of installations is equal to the initial value, namely $S = S0$.

3.3.3. Updating the states of installations

Firstly, whether the installations of leaking state have been ignited is assessed. For domino effects triggered by overpressure, failure time is ignored since the failure caused by overpressure is almost instantaneous. Therefore, the escalation of the domino effect caused by VCE should be prioritized. The specific explanation of this process is as follows:

(1) Updating state transitions by direct ignition

At the initial time ($t = 0$), if there is an installation i at leaking state (denoted as S(i)=1), random sampling is performed based on uniform distribution [0,1] (The random sampling processes applied below are all based on a uniform distribution of [0,1]). If the sampling result falls into the [0, P_1], installation i is immediately ignited, its state transfer to PF, and S (i)=2. Otherwise, the installation is not be ignited immediately.

(2) Updating state transitions by delayed ignition

For time steps where $t \neq 0$, if installation i remains at leaking state (denoted as S(i)=1), whether installation i has been delayed ignited is determined. According to Eq. (1), the ignition probability caused by the ignition source IS within time t can be determined as shown in Eq. (20).

$$P_{\text{Delayed ignition,t}} = P_{IS}(t) - P_{IS}(t - \Delta t) \tag{20}$$

Random sampling is performed, and if the result falls in [0, $P_{\text{Delayed ignition,t}}$], the vapor cloud is ignited. In scenarios involving multiple ignition sources, the vapor cloud is ignited if the sampling result associated with any one ignition source falls in the ignition range. This procedure is repeated until a delayed ignition occurs. Then, the type of accident caused by ignition can be determined through the state transition described in Section 2.1 and random sampling. If the sampling result falls into the [0, P_2], the escalation result will be a VCE and S(i)=3; otherwise, the escalation result will be FF and S(i)=4.

(3) Updating the state of installations damaged by overpressure

Upon ignition, the installation state is updated according to the

Table 3
Critical thermal dose and pool fire duration of each tank.

Tank No.	T1	T2	T3	T4	T5	T6	T7	T8
Critical thermal dose	17,980	17,980	19,219	17,980	17,980	19,219	17,980	17,980
Burning duration (min)	500.7	333.9	66.4	500.7	333.9	44.3	500.7	333.9

Table 4
Thermal radiation intensity (kW/m^2) and explosion overpressure (kPa) between tanks [35].

TRI(kW/m^2)/SWO(kPa) Tank i	Tank j	T1	T2	T3	T4	T5	T6	T7	T8
T1		–	16.5/20.27	4.62/15.51	16.5/9.03	9.04/9.65	3.69/10.14	4.62/6.73	3.69/7.31
T2		16.5/9.03	–	16.5/20.27	9.05/7.03	16.5/9.03	9.05/9.65	3.69/6	4.62/6.72
T3		4.46/5.56	16.7/9.03	–	3.71/4.8	9.11/6.68	16.7/9.03	2.29/3.9	3.71/4.78
T4		16.5/20.27	9.04/41.85	3.69/31.3	–	16.5/20.27	4.62/15.51	16.5/9.03	9.04/9.65
T5		9.05/9.65	16.5/20.27	9.05/41.85	16.5/9.03	–	16.5/20.27	9.05/7.03	16.5/9.03
T6		3.71/5.65	9.11/9.31	16.7/20.82	4.64/5.6	16.7/9.1	–	3.71/4.84	9.11/6.73
T7		4.62/15.51	3.69/31.3	2.28/41.85	16.5/20.27	9.04/41.85	3.69/31.3	–	16.5/20.27
T8		3.69/10.14	4.62/15.51	3.69/31.3	9.05/9.65	16.5/20.27	9.05/41.85	16.5/9.03	–

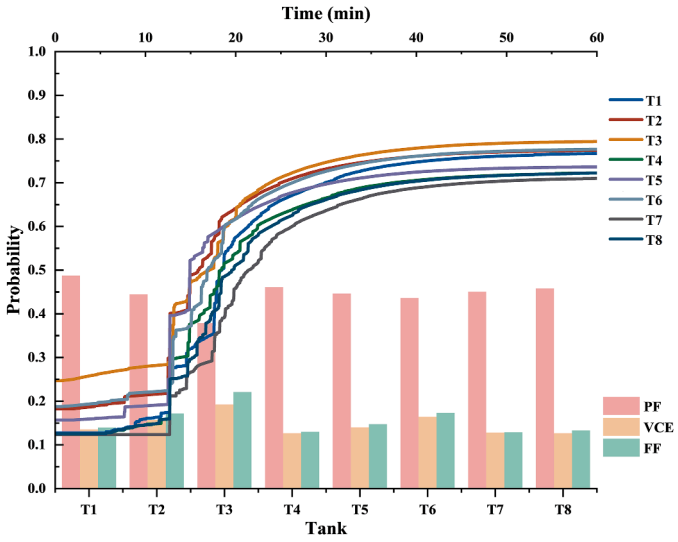

Fig. 9. Dynamic failure probability and accident state of T1-T8 during the evolution of domino effect.

previous accident state. If the state of installation h at the previous time step is VCE (denoted as S(h)=3), whether the VCE will cause an escalation of the tank j at safe state is judged. If SWO(h, j) > Pth(j), the escalation probability **P** is determined according to Eqs. (8)-(12), followed by random sampling. If the sampling result falls into the [0, P], the installation j will fail. Otherwise, it will remain at safe state. Similarly, the state of installation j after failure is determined based on the event tree and random sampling. If the sampling result falls into $[0, P_1^{''}]$, $[P_1^{''}, P_1^{''} + (1 - P_1^{''}) * P_2]$ or $[P_1^{''} + (1 - P_1^{''}) * P_2,\ 1]$, the escalation results are PF, VCE, or FF, respectively. Subsequently, the state of tank h changes to extinguished, which means S(h)=5.

(4) Updating the state of installations damaged by thermal radiation

For the installation j that remains at safe state at time t, the thermal radiation intensity received by installation j at the current time step is firstly calculated and then the accumulated thermal dose is updated. Considering the synergistic effect of multiple fires, the thermal radiation intensity received by installation j can be determined by Eq. (21).

$$Q(j) = \sum_{j,S(j)=0 \text{ and } j\neq i} TRI(k,i) \text{ when } S(k) = 2 \quad (21)$$

The cumulative thermal radiation dose is updated according to Eq. (22).

$$Da(j) = Da(j) + Q(j)^{\alpha} \times \Delta t \quad (22)$$

If the cumulative thermal radiation dose of installation j exceeds the critical value, that is, Da (j) > Dth (j), failure occurs. The type of accident after failure is also determined based on the event tree and random sampling. If the sampling result falls into $[0, P_1^{'}]$, $[P_1^{'}, P_1^{'} + (1 - P_1^{'}) * P_2]$, $[P_1^{'} + (1 - P_1^{'}) * P_2,\ 1]$, the upgrade result is PF, VCE, or FF, respectively.

(5) Updating state transitions by extinguished

For installation k that is at PF state at time t, if the combustion duration exceeds the combustible time, i.e. TD (k) > B (k), then the state of installation k transfers to extinguished, otherwise it sustains the PF state, and TD (k) = TD(k) + ΔT.

3.3.4. *Calculating dynamic domino probabilities*

The escalation time and order are recorded. For each simulation step, count the state of each installation at each time step, and after completing whole simulation, calculate the dynamic domino probability of each installation.

4. Model validation

In the early morning of Sunday, 11 December 2005, a series of explosions and fires destroyed most of the Buncefield Oil Storage and Transfer Depot [67]. This is one of the worst industrial accidents in UK history, which can be used as a suitable case to validate the spatial-temporal evolution model of domino effect.

The accident was caused by overfilling of a large storage tank, resulting in an LOC. After more than 40 min of leakage, a large-scale VCE occurred, followed by a fire involving 23 storage tanks in different bunds. Eyewitness accounts testify that several minor explosions occurred within half an hour of the first explosion, and there is evidence suggesting that the emergency generator and the pump were the most likely ignition sources [67]. The layout of the Buncefield oil depot is shown in Fig. 5, showing the 35 storage tanks that have already been assigned numbers. The diameter and spacing of the tanks can be determined from the scale provided, enabling the calculation of the tanks' parameters based on standard tank dimensions. Tank T2 is where the oil spill took place, with IS1 and IS2 identified as the ignition sources. The hazardous substance involved in the incident was primarily gasoline, a highly flammable and volatile liquid. Fig. 6 illustrates the event tree for the leakage of flammable and volatile liquid materials [59,60,68]. According to Chen et al. [15], the primary ignition probabilities of the two ignition sources are considered 0.1/min (with 'good' ignition controls), resulting in a parameter of ω equal to 0.0018 in Eq. (1). IS1 is active after t = 1.5 min, while IS2 is active at t = 5 min.

For the model validation, 35 storage tanks are firstly identified as the main hazardous installations, and T2 leakage due to LOC is set as the primary accident scenario. Thermal radiation and overpressure are determined according to the method described by Assael and Kakosimos [65]. Fig. 7 illustrates the failure probability of tank T1-T35 and the probabilities of failure state for tanks at t = 45 min. It is clear that over time, the failure probability of tanks continues to rise. Tanks T1-T24 are particularly at risk of failure due to the domino effect before t = 45 min, with their failure probabilities exceeding 0.9 [15]. The accident investigation report confirms damage to tanks T1-T25, except for T5 and T9,

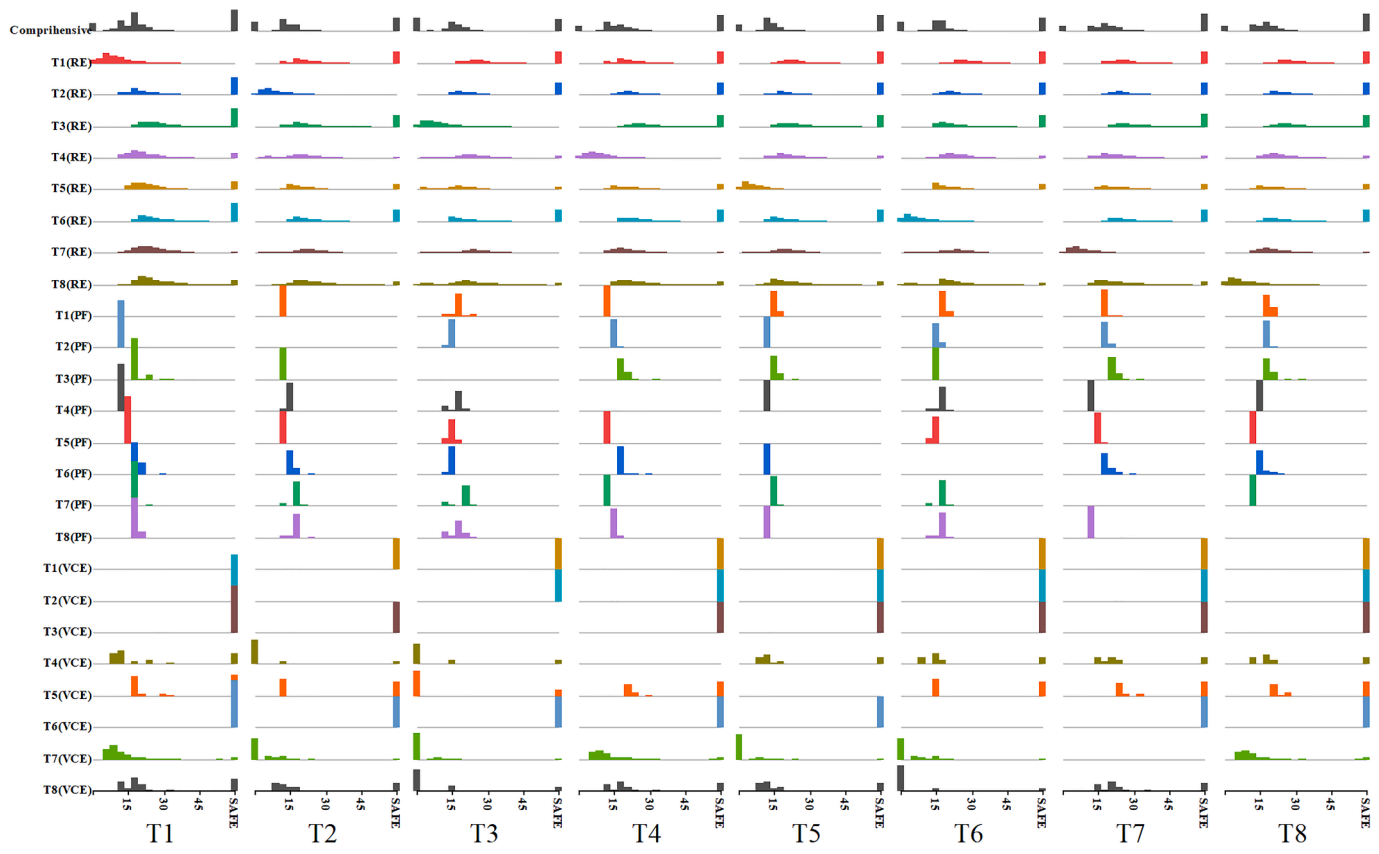

Fig. 10. Distribution of domino effect escalation time for different primary accident scenarios.

Table 5
Top 15 most likely accident chains given a primary PF at tank T5.

Probability	Accident chain
0.08511	T5(PF:0)→T2(PF:12.70),T4(PF:12.70),T8(PF:12.70)→T6(PF:13.03)→T1(PF:14.55),T7(PF:14.55)→T3(PF:14.83)
0.02154	T5(PF:0)→T2(FF:12.70),T4(PF:12.70),T8(PF:12.70)→T6(PF:13.03)→T1(PF:14.55),T7(PF:14.55)→T3(PF:14.83)
0.02139	T5(PF:0)→T2(PF:12.70),T4(PF:12.70),T8(PF:12.70)→T6(PF:13.03)→T1(PF:14.55),T7(PF:14.55)→T3(FF:14.83)
0.02114	T5(PF:0)→T2(PF:12.70),T4(PF:12.70),T8(PF:12.70)→T6(PF:13.03)→T1(FF:14.55),T7(PF:14.55)→T3(PF:14.83)
0.02104	T5(PF:0)→T2(PF:12.70),T4(PF:12.70),T8(PF:12.70)→T6(PF:13.03)→T1(PF:14.55),T7(FF:14.55)→T3(PF:14.83)
0.02101	T5(PF:0)→T2(PF:12.70),T4(FF:12.70),T8(PF:12.70)→T6(PF:13.03)→T1(PF:14.55),T7(PF:14.55)→T3(PF:14.83)
0.02054	T5(PF:0)→T2(PF:12.70),T4(PF:12.70),T8(PF:12.70)→T6(FF:13.03)→T1(PF:14.55),T7(PF:14.55)→T3(PF:14.83)
0.02027	T5(PF:0)→T2(PF:12.70),T4(PF:12.70),T8(FF:12.70)→T6(PF:13.03)→T1(PF:14.55),T7(PF:14.55)→T3(PF:14.83)
0.01451	T5(PF:0)→T2(PF:12.70),T4(PF:12.70),T8(PF:12.70)→T6(VCE:13.03)→T1(PF:14.68),T7(PF:14.68)→T3(PF:15.71)
0.01425	T5(PF:0)→T2(PF:12.70),T4(PF:12.70),T8(PF:12.70)→T6(PF:13.03)→T1(VCE:14.55),T7(PF:14.55)→T3(PF:14.87)
0.01421	T5(PF:0)→T2(VCE:12.70),T4(PF:12.70),T8(PF:12.70)→T6(PF:13.15)→T7(PF:14.72) →T1(PF:15.50)→T3(PF:16.02)
0.01324	T5(PF:0)→T2(PF:12.70),T4(PF:12.70),T8(PF:12.70)→T6(PF:13.03)→T1(PF:14.55),T7(PF:14.55)→T3(VCE:14.83)
0.00727	T5(PF:0)→T2(PF:12.70),T4(PF:12.70),T8(PF:12.70)→T6(PF:13.03)→T1(PF:14.55),T7(VCE:14.55)→T3(FF:14.55*)
0.00625	T5(PF:0)→T2(PF:12.70),T4(VCE:12.70),T8(PF:12.70)→T3(FF:12.70*)→T6(PF:12.95)→T1(PF:15.20)→T7(PF:15.37)
0.00593	T5(PF:0)→T2(PF:12.70),T4(PF:12.70),T8(FF:12.70)→T6(PF:13.03)→T1(PF:14.55),T7(FF:14.55)→T3(PF:14.83)

which aligns closely with the simulation results. This alignment validates the accuracy of the proposed spatial-temporal evolution model of the domino effect in this study.

5. Case study

5.1. Description of case

The model's accuracy was validated through the Buncefield accident case. However, it did not fully showcase the capabilities of the spatial-temporal evolution model of domino effect. Therefore, this section further demonstrates based on the cases provided by Cozzani and Salzano [69], Khakzad et al. [70], and Huang et al. [35]. In this particular scenario, the research area involves of eight atmospheric storage tanks with fixed roofs and one ignition source, the layout is shown in Fig. 8. Assuming the ignition efficiency of the ignition source is also 0.0018. The information of the storage tanks are presented in Table 2. Benzene and toluene are flammable volatile liquids.

To explore the spatial-temporal evolution of domino effect, RE, PF, and VCE [71], are designated as primary accidents in this study. For the scenario of significant RF in tanks, assume a leakage rate of 100 kg/s [1, 30]. According to the vapor cloud dispersion model in Eq. (2), after RFs occur in tanks T1-T8, the ignition source is activate after 3.00 min, 2.07 min, 1.97 min, 2.07 min, 0.83 min, 0.67 min, 1.97 min and 0.83 min, respectively. The critical thermal dose for each tank was determined according to Eq. (5), and the outcomes are presented in Table 3. Additionally, the burning duration and physical effect intensity determined by Huang et al. [35] using ALOHA software are listed in Tables 3 and 4.

5.2. Results and discussion

In this analysis, the primary accident installations (T1-T8) and the primary accident types (RE, PF, and VCE) are considered random. Fig. 9 shows the dynamic failure probability of different tanks due to the domino effect and the probability of each accident type. Under random primary accident conditions, the probability trend of hazardous installations failure is similar. The period 10–20 min after the primary

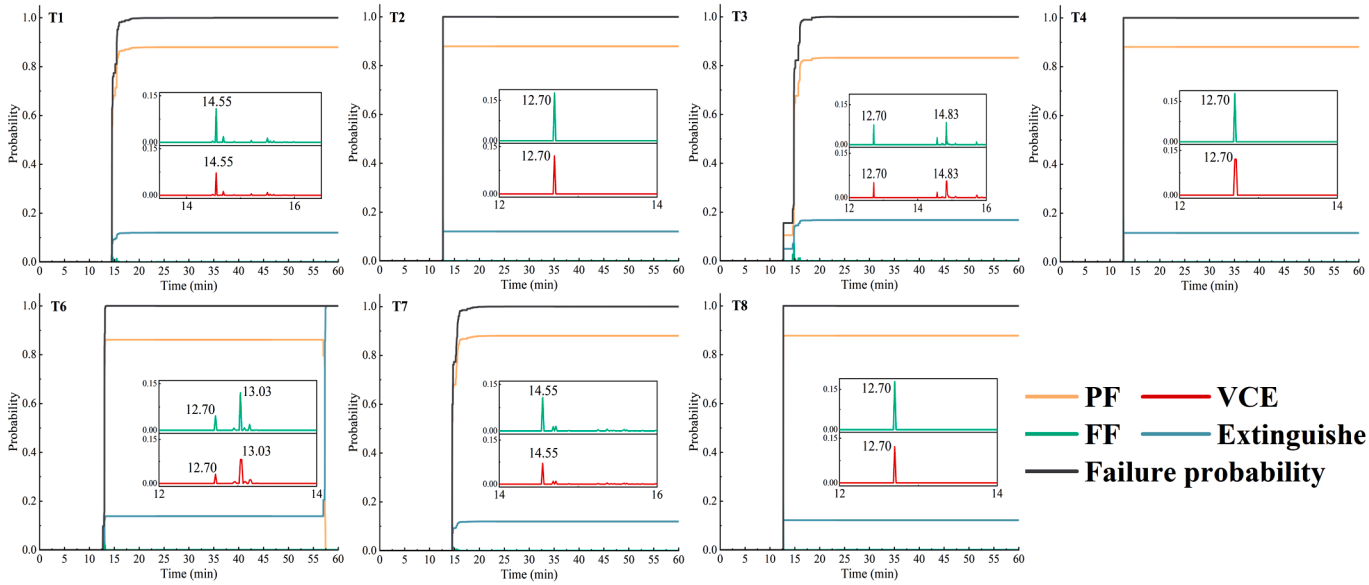

Fig. 11. Dynamic probability of tanks with the primary accident PF at T5.

Table 6
Top 15 most likely accident chains given a primary VCE at tank T7.

Probability	Accident chain
0.00747	T7(VCE:0)→T3(VCE:0*),T5(VCE:0*)
0.00546	T7(VCE:0)→T2(FF:0*),T3(FF:0*), T5(FF:0*),T6(FF:0*)→T1(PF:5.63), T4(PF:5.63), T8(PF:5.63)
0.00542	T7(VCE:0)→T3(VCE:0*)
0.00465	T7(VCE:0)→T3(VCE:0*),T5(VCE:0*),T6(VCE:0*)
0.00443	T7(VCE:0)→T2(VCE:0*),T3(VCE:0*),T5(VCE:0*)
0.00412	T7(VCE:0)
0.00404	T7(VCE:0)→T2(FF:0*),T3(FF:0*),T5(FF:0*)→T6(PF:4.70)→T1 (PF:6.22) →T4(PF:6.31) → T8(PF:6.80)
0.00371	T7(VCE:0)→T3(FF:0*), T5(FF:0*),T6(FF:0*)→T2(PF:4.40)→T8 (PF:6.30) →T4(PF:6.78) → T1(PF:7.45)
0.00368	T7(VCE:0)→T3(VCE:0*),T6(VCE:0*)
0.00362	T7(VCE:0)→T2(FF:0*),T3(VCE:0*),T5(FF:0*),T6(FF:0*)→T8(PF:6.42) →T4(PF:6.43) → T1(PF:6.57)
0.0036	T7(VCE:0)→T2(FF:0*),T3(FF:0*),T5(VCE:0*),T6(FF:0*)→T1(PF:8.00) →T4(PF:9.87) → T8(PF:10.73)
0.0035	T7(VCE:0)→T2(VCE:0*),T3(FF:0*), T5(FF:0*),T6(FF:0*)→T8 (PF:6.63) →T4(PF:7.60) → T1(PF:9.33)
0.00339	T7(VCE:0)→T2(FF:0*),T3(FF:0*),T5(FF:0*),T6(VCE:0*)→T1(PF:6.43) →T4(PF:6.57) → T8(PF:7.47)
0.00332	T7(VCE:0)→T2(VCE:0*),T3(VCE:0*)
0.00314	T7(VCE:0)→T2(VCE:0*),T3(VCE:0*),T5(VCE:0*), T6(VCE:0*)

accidents is a frequent time for domino effect escalation. Fig. 10 shows the distribution of domino effect escalation times under random primary accidents and 24 single primary accidents. Obviously, due to the uncertainty of ignition time, the domino escalation caused by RF as the primary accident has greater uncertainty. When PF is the primary accident, the domino effect escalation times for each tank are more concentrated. When T4 (PF), T4 (VCE), T5 (PF), and T7 (VCE) are the primary accident scenarios, especially the latter two, the accidents progress more rapidly, and tank failures are more concentrated, placing greater pressure on emergency response. Therefore, it is crucial to prioritize the allocation of safety resources towards T4, T5, and T7. Emphasis should be placed on enhancing leakage surveillance for tanks T5 and T7 to strengthen overall safety infrastructure.

Table 5 illustrates the 15 most likely accident sequences, including their ranking and probability, under the assumption that a PF event at tank T7 is the primary accident. Each accident chain details the comprehensive spatial-temporal evolution of domino accidents, including escalation time and accident type. It is assumed that the domino effect triggered by overpressure occurs within a very short time after the explosion. The "*" in the upper right corner of the escalation time indicates this situation.

The most likely domino accident sequence initiated by a PF of tank T5 unfold as follows: T5(PF:0)→T2(PF:12.70),T4(PF:12.70),T8 (PF:12.70)→T6(PF:13.03)→T1(PF:14.55),T7(PF:14.55)→T3(PF:14.83). The probability of this sequence is 0.08511. To provide a detailed insight into the spatial-temporal evolution, the accident chain is analyzed: T5 (PF:0)→T2(PF:12.70),T4(VCE:12.70),T8(PF:12.70)→T3(FF:12.70*)→ T6(PF:12.95)→T1(PF:15.20)→T7(PF:15.37). At the initial time (t = 0 min), the primary PF occurs in tank T5. Following this event, the target installations T1-T4 and T6-T8 are exposed to continuous thermal radiation from tank T5. Among these tanks, the thermal dose accumulation of tanks T2, T4 and T8 reaches its peak value initially at $t = 12.70$ min, leading to the first failure. The VCE in T4 results in an overpressure of 31.3 kPa on tank T3, surpassing the threshold of 22 kPa, indicating potential escalation. In this sequence, tank T3 fails due to explosion overpressure, causing an FF event. After T4 is extinguished and T3 transforms into PF, the synergistic effect of T2, T3, T5, and T8 accelerates the domino accident evolution. Ultimately, T6, T1, and T7 experience an escalation of the domino effect at $t = 12.95$ min, $t = 15.20$ min, and $t = 15.37$ min, respectively.

Among the 15 most likely accident sequences outlined in Table 5, the sequence of escalation in the majority of accident chains remains consistent. The dynamic failure probability effectively showcases the failure trend of each tank. In the domino scenario where the primary accident involves PF at tank T5, the dynamic failure probabilities and accident state probabilities of other tanks are shown in Fig. 11. The approximate time for each tank to experience an accident can be obtained from the accident chain or dynamic probability diagrams. For example, tank T3 primarily occurs domino escalation at two pivotal time points or periods: $t = 12.70$ min and $t = 14.83$ min. The results further indicate the sequence of domino propagation is roughly from T2, T4, T8, T6, T1, T7 to T3, which aligns with the proximity to the primary accident tank. Closer tanks receive stronger thermal radiation, contributing to this order. Therefore, in emergency response planning, besides addressing the fire in T5, priority should be given to allocating emergency resources to T2, T4, and T8. This allocation strategy can effectively mitigate the heat accumulation in T2, T4 and T8, thus, controlling the spread of the domino effect.

If a VCE occurs at tank T7 as the primary accident, the spatial-temporal evolution of the domino effect becomes more complex. As

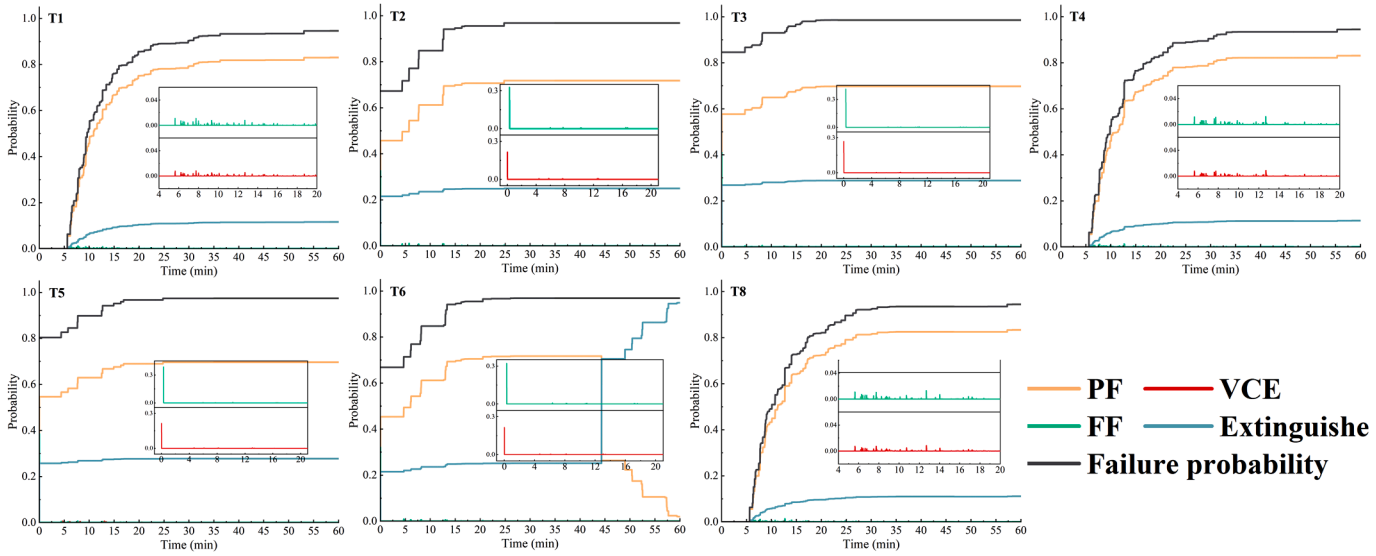

Fig. 12. Dynamic probability of tanks with the primary accident VCE at T7.

shown in Table 6, it outlines the 15 most likely accident sequences and their probabilities under this primary accident scenario. The most likely sequence observed is T7(VCE:0) →T3(VCE:0*), T5(VCE:0*). Alongside the most likely accident chain, which only includes first-order domino effects, there are sequences that involving higher-order domino effects. For instance, T7(VCE:0)→T2(FF:0*),T3(FF:0*), T5(FF:0*),T6(FF:0*)→T1(PF:5.63),T4(PF:5.63), T8(PF:5.63) or T7(VCE:0)→T2(FF:0*),T3(FF:0*),T5(FF:0*)→T6(PF:4.70)→T1(PF:6.22)→T4 (PF:6.31)→T8 (PF:6.80). Between the 10th to 13th accident chains, the sequential evolution of the domino effect remains constant, but the escalation time is quite different. These case scenarios show that the domino effect triggered by a VCE present more complexity compared with that induced by a PF.

Fig. 12 present tank failure and dynamic state probabilities. When comparing Fig. 11, it's apparent that the evolution of domino effect becomes substantially more complex and rapid with a VCE as the initiating accident. The diffusion of vapor cloud is influenced by wind direction and speed, the approximate evolution sequence of the domino effect is T3, T5, T2, T6, T4, T8, and T1. The tanks located downwind will fail at an easier stage in this sequence.

Primary scenarios involving multiple installations cannot be overlooked compared to scenarios where only one installation is damaged, which are likely to occur in extreme natural disasters or terrorist attacks [22,35,63]. The fire and explosion accidents caused by hurricane Harvey and the Great East Japan earthquake have emphasized that multiple primary accidents must be addressed as a major concern.

The appendix provides the time distribution of domino effect escalation in hazardous installations under multiple primary accident scenarios. The synergistic effect of multiple accidents significantly increases the destructive power of primary accidents. When multiple PFs are used as primary accident scenarios, the intensity of thermal radiation received by the target tank is increased, which advances the time for reaching the critical thermal dose and causing domino escalation. According to the escalation time distribution, the domino effect scenarios caused by the multiple primary accident scenarios including VCE are still more complicated. Among them, the evolution process of the domino effect is faster in the scenarios of T7(VCE)+T4(VCE), T7(VCE)+T5(PF), T7(VCE)+T6(PF), T7(VCE)+T8(PF) and T7(VCE)+T8(VCE).

Fig. 13 shows the dynamic failure probability of different target installations under these primary accident scenarios. Compared to a single primary accident, multiple primary accidents accelerate the evolution of the domino effect, requiring quicker emergency response times and more emergency supplies. The exception is if a VCE is the primary accident. If the explosion overpressure on surrounding hazardous installations does not cause the domino effect to escalate, this situation will slow down the evolution of the domino effect. For example, in Fig. 13, when T5 (PF) + T2 (VCE) is the primary accident scenario, T2 (VCE) will not cause a domino effect. In this case, the domino escalation time of T1 and T3 may be slower than that of T5 (PF) as the primary accident scenario.

To further compare the influence of PF or VCE as the primary accident on the evolution of the domino effect, five additional primary accident scenarios are added to the existing settings of T5(PF), T7(VCE), and T7(VCE)+T5(PF). These scenarios are T5(VCE), T7(PF), T5(PF)+T7(PF), T5(VCE)+T7(VCE), and T5(VCE)+T7(PF). This allows for a comparative analysis of the accident types in the domino evolution process. Fig. 14 illustrates the probability of PF, VCE, and FF occurring in the other six tanks across these eight primary accident conditions. Comparisons indicate that when T5(PF), T7(PF) or T5(PF)+T7(PF) are set as the primary accidents, there is little variation in the probability of the three types of accidents (PF, VCE, FF) occurring in the other six tanks. This aligns with the accident tree, where the highest probability of a domino escalation induced by thermal radiation is either PF or FF. Additionally, FF can transfer to PF, leading further escalations due to thermal radiation. In contrast, when primary accidents involve VCE, the probabilities of PF, VCE, and FF in the other six tanks display significant differences. This is tied to whether the overpressure from tank T5 and T7 explosions exceeds the escalation threshold on the other six storage tanks. It also signifies that the VCE as a primary accident enhance the complexity of accident chains, which is consistent with the previous analysis. Comparing single primary accident scenarios with multiple primary accident scenarios, it is evident that under multiple primary accident conditions, the discrepancy in PF, VCE, and FF in the other six tanks after the failure due to the domino effect is more significant. This indicates that multiple accidents amplify the complexity of the domino accidents. In conclusion, multiple primary accident scenarios present greater challenges for the emergency response to domino accidents.

6. Conclusions

The domino effect is a significant concern in chemical industry risk assessments, characterized by spatial-temporal complexity and uncertainty in the accident evolution process. In this work, a new spatial-temporal evolution of domino effects has been proposed to simulate the sequence of domino accidents and calculate the corresponding probabilities. This study introduces the concept of critical thermal dose

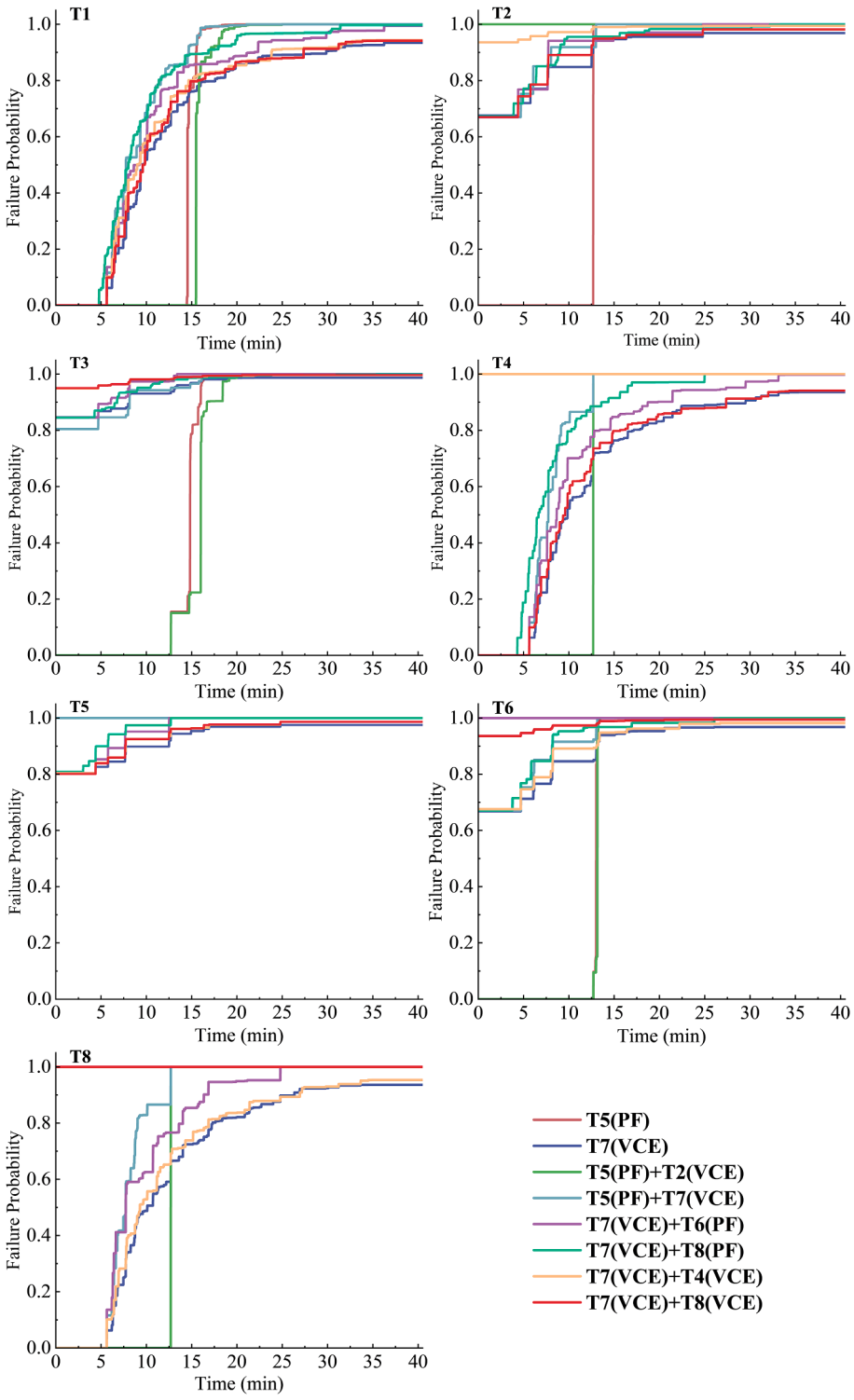

Fig. 13. Failure probability of tanks under different primary accidents.

as a failure criterion for storage tanks exposed to fire accidents and combines it with the Probit model to enhance assessments of domino escalation. Comparison of the failure times calculated by the critical thermal dose method with the results of FEA showed an error within 15%, and the error for further comparison of the evolution process did not exceed 3.4%. The accuracy of the critical thermal dose method is validated.

A Monte Carlo-based modeling approach enhances the applicability of spatial-temporal evolution model for high order, multi-accident type domino accidents, and the effectiveness of this model is verified by accident cases. The case study demonstrates that the proposed model can characterize the state transition of multiple accident types in the spatial-temporal dimension and overcome the limitations of probabilistic modeling at a high order of propagation. The accident chains, evolution

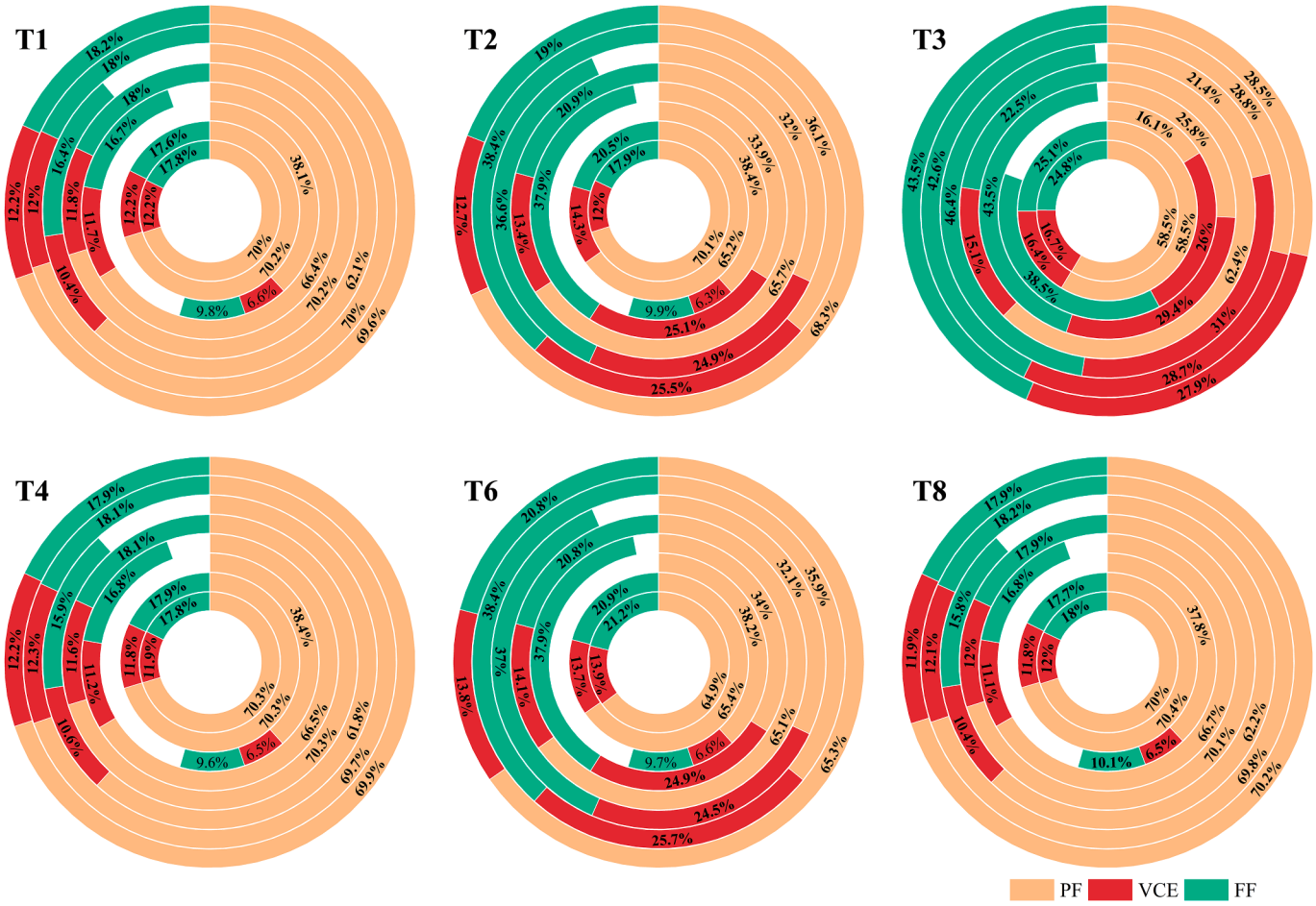

Fig. 14. Probability of domino escalation to PF, VCE, FF (From the inside out, the primary accidents are (T5(PF), T7(PF), T5(VCE), T7(VCE), T5(PF)+T7(PF), T5(VCE)+T7(VCE), T5(PF)+T7(VCE) and T5(VCE)+T7(PF)).

times and dynamic failure probabilities of hazardous installations obtained based on this evolutionary modeling aid in risk assessment and the creation of targeted prevention strategies. Analysis indicates that emergency resources should be prioritized and allocated to T4, T5 and T7 to mitigate the severity of the subsequent domino effect. Additionally, the evolution of domino accidents resulting from the primary accident at the explosion is more complex and the domino effect caused by multiple primary accidents cannot be disregarded.

In summary, the study's advancements significantly enhance the accuracy of risk assessment and contribute to the development of more effective measures for preventing and mitigating chemical process accidents, offering a deeper insight into the domino effect's dynamics. One challenge remains in managing the vast array of potential accident chains generated by the model. Establishing criteria for selecting the most probable and severe sequences is essential for practical application.

CRediT authorship contribution statement

Weikai Ma: Writing – original draft, Validation, Software, Methodology, Formal analysis, Data curation. **Yanfu Wang:** Writing – review & editing, Writing – original draft, Funding acquisition, Formal analysis. **Peijie Xing:** Writing – original draft, Software. **Ming Yang:** Writing – review & editing, Validation, Supervision.

Declaration of competing interest

The authors declare no conflict of interests.

Data availability

No data was used for the research described in the article.

Acknowledgment

This work is supported by Research Project of "National Natural Science Foundation of China (Grant no. 52171353)", "the Fundamental Research Funds for the Central Universities (No. 24CX02024A)", "Special Fund for the Technology-Benefiting-People Program in Qingdao (No. 21–1–4-sf-3-nsh)", and the Open Project of the State Key Laboratory of Chemical Safety. This research has received funding from the European Union's Horizon 2020 research and innovation program under the Marie Skłodowska-Curie grant agreement H2020-MSCA-IF-2018–840425.

Appendix A. Distribution of domino effect escalation time under multiple primary accident scenarios

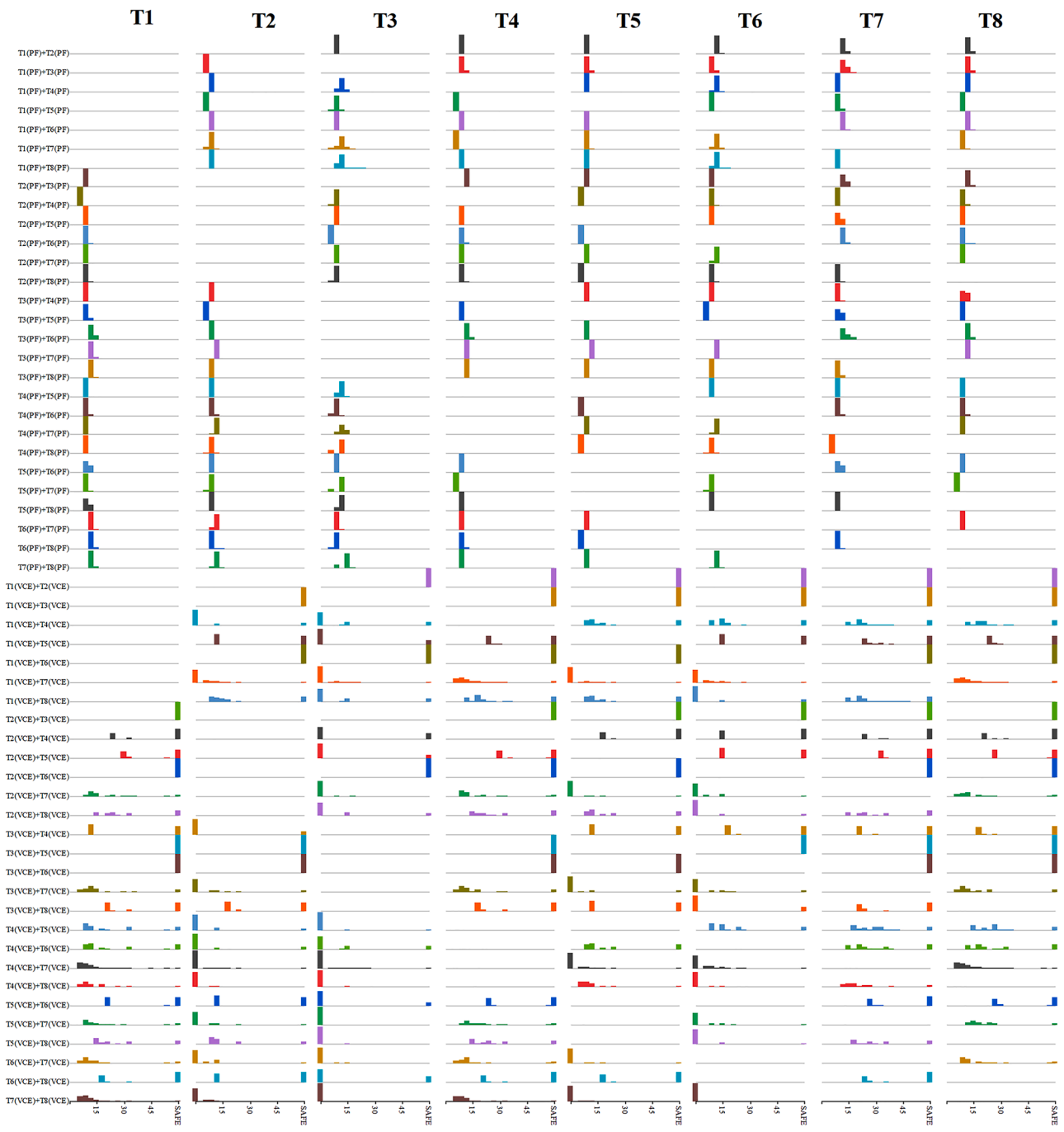

Fig. A1. Distribution of domino effect escalation time under multiple primary accident scenarios.

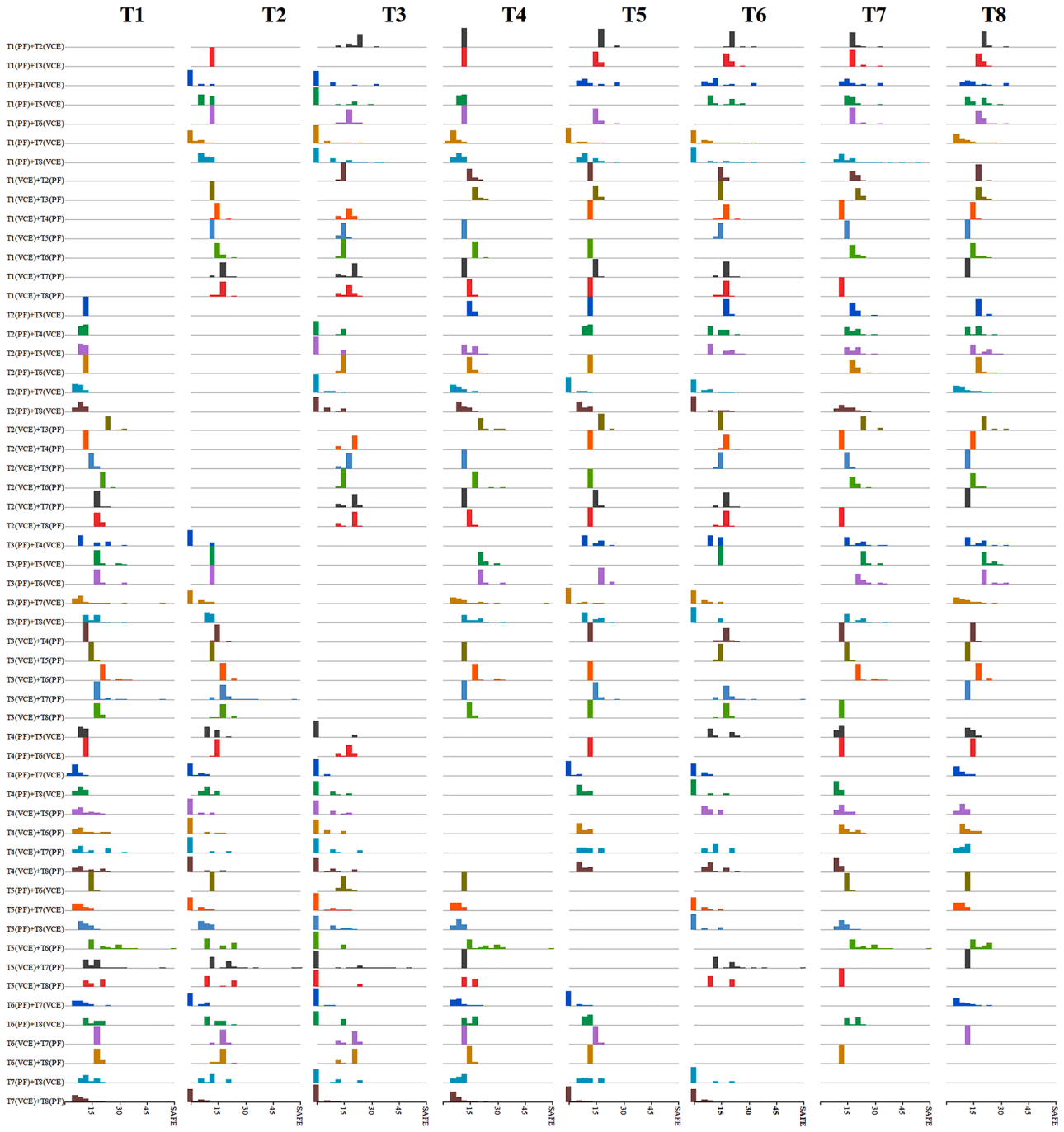

Fig. A1. (*continued*).

References

[1] Chen C, Reniers G, Khakzad N. A dynamic multi-agent approach for modeling the evolution of multi-hazard accident scenarios in chemical plants. Reliab Eng Syst Saf 2021;207:14.

[2] Reniers GLL, Sörensen K, Khan F, Amyotte P. Resilience of chemical industrial areas through attenuation-based security. Reliab Eng Syst Saf 2014;131:94–101.

[3] Guo C, Khan F, Imtiaz S. Copula-based Bayesian network model for process system risk assessment. Process Saf Environ Protect 2019;123:317–26.

[4] Khakzad N. Application of dynamic Bayesian network to risk analysis of domino effects in chemical infrastructures. Reliab Eng Syst Saf 2015;138:263–72.

[5] Amin MT, Scarponi GE, Cozzani V, Khan F. Improved pool fire-initiated domino effect assessment in atmospheric tank farms using structural response. Reliab Eng Syst Saf 2024;242:109751.

[6] Huang KX, Chen GH, Khan F, Yang YF. Dynamic analysis for fire-induced domino effects in chemical process industries. Process Saf Environ Protect 2021;148:686–97.

[7] Li XF, Chen GH, Amyotte P, Alauddin M, Khan F. Modeling and analysis of domino effect in petrochemical storage tank farms under the synergistic effect of explosion and fire. Process Saf Environ Protect 2023;176:706–15.

[8] Darbra RM, Palacios A, Casal J. Domino effect in chemical accidents: main features and accident sequences. J Hazard Mater 2010;183:565–73.

[9] Tamascelli N, Scarponi GE, Amin MT, Sajid Z, Paltrinieri N, Khan F, et al. A neural network approach to predict the time-to-failure of atmospheric tanks exposed to external fire. Reliab Eng Syst Saf 2024;245:109974.

[10] Lan M, Gardoni P, Qin RS, Zhang X, Zhu JP, Lo SM. Modeling NaTech-related domino effects in process clusters: a network-based approach. Reliab Eng Syst Saf 2022;221:16.

[11] Hou L, Wu XG, Wu Z, Wu SZ. Pattern identification and risk prediction of domino effect based on data mining methods for accidents occurred in the tank farm. Reliab Eng Syst Saf 2020;193:10.

[12] Xie SY, Dong SH, Chen YN, Peng YJ, Li XC. A novel risk evaluation method for fire and explosion accidents in oil depots using bow-tie analysis and risk matrix analysis method based on cloud model theory. Reliab Eng Syst Saf 2021;215:18.

[13] Khakzad N, Amyotte P, Cozzani V, Reniers G, Pasman H. How to address model uncertainty in the escalation of domino effects? J Loss Prev Process Ind 2018;54:49–56.
[14] Xu YY, Reniers G, Yang M, Yuan SQ, Chen C. Uncertainties and their treatment in the quantitative risk assessment of domino effects: classification and review. Process Saf Environ Protect 2023;172:971–85.
[15] Chen C, Khakzad N, Reniers G. Dynamic vulnerability assessment of process plants with respect to vapor cloud explosions. Reliab Eng Syst Saf 2020;200:15.
[16] Huang KX, Chen GH, Khan F. Vulnerability assessment method for domino effects analysis in chemical clusters. Process Saf Environ Protect 2022;164:539–54.
[17] Salzano E, Cozzani V. The analysis of domino accidents triggered by vapor cloud explosions. Reliab Eng Syst Saf 2005;90:271–84.
[18] Khan FI, Abbasi SA. Models for domino effect analysis in chemical process industries. Process Saf Prog 1998;17:107–23.
[19] Marroni G, Casini L, Bartolucci A, Kuipers S, Moreno VC, Landucci G. Development of fragility models for process equipment affected by physical security attacks. Reliab Eng Syst Saf 2024;243:18.
[20] Cui XM, Zhang MG, Pan WJ. Dynamic probability analysis on accident chain of atmospheric tank farm based on Bayesian network. Process Saf Environ Protect 2022;158:146–58.
[21] Zeng T, Chen G, Yang Y, Chen P, Reniers G. Developing an advanced dynamic risk analysis method for fire-related domino effects. Process Saf Environ Protect 2020;134:149–60.
[22] Chen C, Reniers G, Khakzad N. Integrating safety and security resources to protect chemical industrial parks from man-made domino effects: a dynamic graph approach. Reliab Eng Syst Saf 2019;191:13.
[23] Lan M, Gardoni P, Weng WG, Shen KX, He ZC, Pan RL. Modeling the evolution of industrial accidents triggered by natural disasters using dynamic graphs: a case study of typhoon-induced domino accidents in storage tank areas. Reliab Eng Syst Saf 2024;241:15.
[24] Zhou JF, Reniers G. Probabilistic Petri-net addition enabling decision making depending on situational change: the case of emergency response to fuel tank farm fire. Reliab Eng Syst Saf 2020;200:12.
[25] Kamil MZ, Taleb-Berrouane M, Khan F, Ahmed S. Dynamic domino effect risk assessment using Petri-nets. Process Saf Environ Protect 2019;124:308–16.
[26] Zhou J, Reniers G. Dynamic analysis of fire induced domino effects to optimize emergency response policies in the chemical and process industry. J Loss Prev Process Ind 2022;79:104835.
[27] Hashemi SJ, Khan F, Ahmed S. Multivariate probabilistic safety analysis of process facilities using the Copula Bayesian Network model. Comput Chem Eng 2016;93:128–42.
[28] Ovidi F, Zhang LB, Landucci G, Reniers G. Agent-based model and simulation of mitigated domino scenarios in chemical tank farms. Reliab Eng Syst Saf 2021;209:16.
[29] Zhang LB, Landucci G, Reniers G, Khakzad N, Zhou JF. DAMS: a Model to Assess Domino Effects by Using Agent-Based Modeling and Simulation. Risk Anal 2018;38:1585–600.
[30] Gholamizadeh K, Zarei E, Yazdi M, Ramezanifar E, Aliabadi MM. A hybrid model for dynamic analysis of domino effects in chemical process industries. Reliab Eng Syst Saf 2024;241:24.
[31] Zhou LX, Chen GH, Zheng MB, Gao XM, Luo CN, Rao XH. Agent-based modeling methodology and temporal simulation for Natech events in chemical clusters. Reliab Eng Syst Saf 2024;243:16.
[32] Tan X, Xiao S, Yang Y, Khakzad N, Reniers G, Chen C. An agent-based resilience model of oil tank farms exposed to earthquakes. Reliab Eng Syst Saf 2024;247:110096.
[33] Rad A, Abdolharnidzadeh B, Abbasi T, Rashtchian D. FREEDOM II: an improved methodology to assess domino effect frequency using simulation techniques. Process Saf Environ Protect 2014;92:714–22.
[34] Abdolhamidzadeh B, Abbasi T, Rashtchian D, Abbasi SA. A new method for assessing domino effect in chemical process industry. J Hazard Mater 2010;182:416–26.
[35] Huang W, Chen XW. Qin Y. A simulation method for the dynamic evolution of domino accidents in chemical industrial parks. Process Saf Environ Protect 2022;168:96–113.
[36] Li Y, Wang Y, Lai Y, Shuai J, Zhang L. Monte Carlo-based quantitative risk assessment of parking areas for vehicles carrying hazardous chemicals. Reliab Eng Syst Saf 2023;231:109010.
[37] Men JK, Chen GH, Yang YF, Reniers G. An event-driven probabilistic methodology for modeling the spatial-temporal evolution of natural hazard-induced domino chain in chemical industrial parks. Reliab Eng Syst Saf 2022;226:14.
[38] Amin MT, Khan F, Zuo MJ. A bibliometric analysis of process system failure and reliability literature. Eng Fail Anal 2019;106:104152.
[39] Chen C, Reniers G, Khakzad N. A thorough classification and discussion of approaches for modeling and managing domino effects in the process industries. Saf Sci 2020;125:23.
[40] Li XF, Chen GH, Huang KX, Zeng T, Zhang XY, Yang P, et al. Consequence modeling and domino effects analysis of synergistic effect for pool fires based on computational fluid dynamic. Process Saf Environ Protect 2021;156:21.
[41] Wang XZ, Zhou KB, Mebarki A, Jiang JC. Numerical simulation of thermal response behavior of floating-roof tanks exposed to pool fire. Appl Therm Eng 2020;179:14.
[42] Li YH, Jiang JC, Yu Y, Wang ZR, Xing ZX, Zhang QW. Thermal buckling of oil-filled fixed-roof tanks subjected to heat radiation by a burning tank. Eng Fail Anal 2022;138:15.
[43] Pourkeramat A, Daneshmehr A, Jalili S, Aminfar K. Investigation of wind and smoke concentration effects on thermal instability of cylindrical tanks with fixed roof subjected to an adjacent fire. Thin-Walled Struct 2021;160:23.
[44] Landucci G, Gubinelli G, Antonioni G, Cozzani V. The assessment of the damage probability of storage tanks in domino events triggered by fire. Accid Anal Prev 2009;41:1206–15.
[45] Wu Z, Hou L, Wu SZ, Wu XG, Liu FY. The time-to-failure assessment of large crude oil storage tank exposed to pool fire. Fire Saf J 2020;117:13.
[46] Yang JH, Zhang MG, Zuo YW, Cui XM, Liang CQ. Improved models of failure time for atmospheric tanks under the coupling effect of multiple pool fires. J Loss Prev Process Ind 2023;81:10.
[47] Yang JF, Zhang B, Chen LC, Diao X, Hu YH, Suo GY, et al. Improved solid radiation model for thermal response in large crude oil tanks. Energy 2023;284:14.
[48] Amin MT, Scarponi GE, Cozzani V, Khan F. Dynamic Domino Effect Assessment (D2EA) in tank farms using a machine learning-based approach. Comput Chem Eng 2024;181:108556.
[49] Ding L, Khan F, Abbassi R, Ji J. FSEM: an approach to model contribution of synergistic effect of fires for domino effects. Reliab Eng Syst Saf 2019;189:271–8.
[50] Ding L, Khan F, Ji J. A novel approach for domino effects modeling and risk analysis based on synergistic effect and accident evidence. Reliab Eng Syst Saf 2020;203:12.
[51] Zhou JF, Reniers G, Cozzani V. Improved probit models to assess equipment failure caused by domino effect accounting for dynamic and synergistic effects of multiple fires. Process Saf Environ Protect 2021;154:306–14.
[52] Zeng T, Wei L, Reniers G, Chen G. A comprehensive study for probability prediction of domino effects considering synergistic effects. Reliab Eng Syst Saf 2024;251:110318.
[53] Ding L, Ji J, Khan F. Combining uncertainty reasoning and deterministic modeling for risk analysis of fire-induced domino effects. Saf Sci 2020;129:9.
[54] Hou SY, Luan XY, Wang Z, Cozzani V, Zhang B. A quantitative risk assessment framework for domino accidents caused by double pool fires. J Loss Prev Process Ind 2022;79:11.
[55] Vilchez JA, Espejo V, Casal J. Generic event trees and probabilities for the release of different types of hazardous materials. J Loss Prev Process Ind 2011;24:281–7.
[56] Ricci F, Yang M, Reniers G, Cozzani V. Emergency response in cascading scenarios triggered by natural events. Reliab Eng Syst Saf 2024;243:16.
[57] Cozzani V, Gubinelli G, Antonioni G, Spadoni G, Zanelli S. The assessment of risk caused by domino effect in quantitative area risk analysis. J Hazard Mater 2005;127:14–30.
[58] Cozzani V, Gubinelli G, Salzano E. Escalation thresholds in the assessment of domino accidental events. J Hazard Mater 2006;129:1–21.
[59] Haag D, P U, Ale BJ. Guidelines for quantitative risk assessment: purple book. The Hague: Advisory Council on Dangerous Substances; 2005.
[60] BEVI. BEVI Reference Manual version 3.2: bilthoven: RVIM; 2009.
[61] Atkinson G. Development of heavy vapour clouds in very low wind speeds. J Loss Prev Process Ind 2017;48:162–72.
[62] Cozzani V, Salzano E. The quantitative assessment of domino effects caused by overpressure - Part I. Probit models. J Hazard Mater 2004;107:67–80.
[63] Chen C, Reniers G, Zhang LB. An innovative methodology for quickly modeling the spatial-temporal evolution of domino accidents triggered by fire. J Loss Prev Process Ind 2018;54:312–24.
[64] Liang CQ, Zhang MG, Zhu JJ, Zuo YW, Yang JH, Cui XM. Escalation probabilistic model of atmospheric tank under coupling effect of thermal radiation and blast wave in domino accidents. J Loss Prev Process Ind 2022;80:12.
[65] Assael MJ, Kakosimos KE. Fires, explosions, and toxic gas dispersions: effects calculation and risk analysis. Boca Raton: CRC Press/Taylor & Francis; 2010.
[66] Jiao Y, Chen R, Wang K, Fan XH, Liu FQ. Simulation of scenario characteristics of LPG tank explosion accident and its contribution to emergency planning: a case study. J Loss Prev Process Ind 2023;83.
[67] Board BMII. The Buncefield incident, 11 December 2005: the final report of the Major Incident Investigation Board: Health and Safety Executive. 2008.
[68] Alileche N, Olivier D, Estel L, Cozzani V. Analysis of domino effect in the process industry using the event tree method. Saf Sci 2017;97:10–9.
[69] Cozzani V, Salzano E. The quantitative assessment of domino effect caused by overpressure - Part II. Case studies. J Hazard Mater 2004;107:81–94.
[70] Khakzad N, Khan F, Amyotte P, Cozzani V. Domino Effect Analysis Using Bayesian Networks. Risk Anal 2013;33:292–306.
[71] He Z, Shen K, Lan M, Weng W. An evacuation path planning method for multi-hazard accidents in chemical industries based on risk perception. Reliab Eng Syst Saf 2024;244:109912.